Table of Contents. Page

Table S1. Influenza A (PR8) peptide analysis. Peptides in **bold** were detected, other peptides were checked but not found. [#] IC_{50} calculated by netMHCpan 2.8 (1), * highly conserved peptides, [†]quantitation by multiple methods (see Supplement, Quantitation), [‡]quantitation relative to other IAV peptides eluting in same region (see Supplement, Quantitation).

Flu Peptide	Source	IC_{50}[#]	Peptide length	Estimated Copies/Cell
FMYSDFHFI*	PA_{46-54}	2.41	9	5
LLIEGTASL	$PB1_{395-403}$	4.04	9	
MQFSSFTV*	$PB2_{630-637}$	4.34	8	
FLDIWTYNA	$HA_{431-439}$	5.22	9	
YMLERELV	$PB2_{204-211}$	5.56	8	
LLTEVETYV*	$M1_{3-11}$	6.72	9	0.5
YLLSWKQV	$PA_{333-340}$	7.03	8	
SLLTEVETYV	$M1_{2-11}$	7.12	10	
FSMELPSFGV	$PB1_{505-514}$	7.39	10	
FMQALHLL*	$NS2_{98-105}$	7.58	8	
LLMDALKLSI	$PA_{283-292}$	8.54	10	
ILPDMTPSI	$PB2_{463-471}$	8.65	9	19
SMIEAESSV	$PA_{594-602}$	9.03	9	
YLLSWKQVL	$PA_{333-341}$	9.20	9	
YIMKGVYI	$PA_{457-464}$	9.34	8	
NMLSTVLGV*	$PB1_{413-421}$	9.40	9	3
FMQALHLLL	$NS2_{99-108}$	9.74	9	
FQNWGVEPI	$PB2_{446-454}$	11.53	9	
LLLEVEQEI	$NS2_{105-113}$	12.93	9	
FVANFSMEL*	$PB1_{501-509}$	13.00	9	
RLIDFLKDV	$PB1_{162-170}$	13.55	9	
GILGFVFTL*	$M1_{58-66}$	15.03	9	650-1000[†]
FLLMDALKL	$PA_{282-290}$	15.42	9	
IILKANFSV	$NS1_{128-136}$	19.35	9	
GLISLILQI	NA_{18-26}	20.27	9	
KVLFQNWGV	$PB2_{443-451}$	22.06	9	
RMGAVTTEV	$M1_{134-142}$	28.24	9	117
FQGRGVFEL	$NP_{458-466}$	28.42	9	
LLTEVETPI*	$M2_{3-11}$	31.21	9	
KLLLIVQAL	$PA_{664-672}$	32.25	9	
NLYQNENAYV	$HA_{206-215}$	37.02	10	
AIMDKNIIL	$NS1_{122-130}$	167.31	9	20-60[‡]
ILGFVFTL*	$M1_{59-66}$	59.36	8	

Materials and Methods Supplemental Information

Affinity isolation and acid extraction of A2 peptides for MS^3 and DIAMS experiments. 10 μg of anti-HLA-A02 BB7.2 mAb (BD Biosciences or Santa Cruz) was non-covalently coupled to 20 μl of Gamma Bind beads (GE Biosciences) for 1 h at room temperature. Post infection, adherent BEAS cells (1-5x10^6) were removed using a cell scraper, pelleted and lysed. Cleared supernatant was incubated with 20 μl of beads for 3 h at 4°C. Beads were washed, fluid aspirated and wet beads stored at -80°C. For MS analysis the beads were incubated with 10% acetic acid at 65°C for 4 minutes, and released peptides trapped on a C18 tip. The tip was eluted into 2-4 μl 60% methanol in water with 0.2% formic. For MS^3 this was loaded into a nanospray needle. For LC-DIAMS this was air dried to 0.25 μl, 2 μl 0.2% TFA was added and this pressure bomb loaded onto the pre-column.

Lung epithelial cells, cell lines and influenza infection. Large T antigen transformed bronchial epithelial BEAS-2B cells (2) purchased from ATCC© did not express surface HLA-A2 by flow cytometric analysis and so were transfected using an HLA-A*02:01 cDNA insert (BEAS cells). We transfected BEAS cells using lipofectamine reagent (Invitrogen) with 2μg of pIRES-Bleo vector with HLA-A*02:01 cDNA insert ($A2^+$-BEAS). Two days post transfection, BEAS cells were stained with FITC-labeled BB7.2 anti-HLA-A02 antibody (BD Biosciences) and positive cells were sorted using a FACSAria™ cell sorter (BD Biosciences). Five rounds of cell sorting were required to select a stably high HLA-A*02:01 expressing BEAS cell line that was used in our experiments. BEAS lacking A2 were also used ($A2^-$-BEAS) when indicated. BEAS cells were grown to semi-confluency on DMEM complete medium (DMEM supplemented with 20% FCS, 2 mM L-glutamine, 1% pen-strep solution, 1 mM sodium pyruvate and 1:1000 tissue culture grade 2-mercaptoethanol (Gibco). BEAS cells were dissociated from culture flasks using trypsin (Gibco) and washed with OptiMEM media (Gibco). Cell pellets were infected using 10 EID_{50} units/cells of influenza A/PR8/34 virus (Charles River Laboratories, Inc.) in 100 μl of OptiMEM media. After 1 h of infection in small volume (500μl), cells were plated on tissue culture flasks and incubated at 37°C in a humidified 5% CO_2 incubator for 6-18 h. Normal human bronchial epithelial (NHBE) cells from Lonza tested as BB7.2 reactive were used in designated experiments. NHBE cells were cultured in complete Bronchial Epithelial Cell Growth Medium (BEGM™, Lonza) for ten generations and harvested using trypsin. NHBE cells were infected and plated as described above for BEAS-2B cells.

Assessing IAV infection by intracellular M1 staining, microscopy and HA staining. Infected lung epithelium cells were harvested using a cell scraper (Corning) at the indicated time points. Cells were fixed and permeated using BD Cytofix/Cytoperm™ buffer according to manufacturer's protocol. Cells were first stained with anti influenza A/M1 (156-02, Santa Cruz) antibody. After 60 min incubation, cells were washed with Cytoperm buffer and stained for an additional 60 min using FITC-labeled Goat anti-mouse IgG (ab6785 Abcam). Cells were washed twice with Cytoperm buffer and fixed using 4% paraformaldehyde (Sigma). Fixed cells were analyzed using FACSAria™ flowcytometer and MoFlow™ program. For microscopy, cells were grown and infected in chamber slides (LabTech Thermo-Fisher Scientific) and washed with PBS, then fixed with Acetone-Methanol Fixative for 20 min. Slides were blocked using 5% FBS 0.3% Triton X-100 in PBS for an hour. Fixed and blocked cells were stained with anti-influenza A/M1 (156-02, Santa Cruz) antibody overnight in 4C° in 2% FBS 0.3% Triton X 100, PBS buffer. Slides were washed and stained at room temp for 60 min using FITC-labeled goat anti-mouse IgG

(ab6785 abcam). Slides were washed and covered with Vectra shield mounting media (Vector Lab). Images were acquired using a Nikon Fluorescence microscope (Nikon Japan) equipped with Spot™ camera (SPOT™ imaging solutions). For HA staining, infected cells were surface stained with PY102 antibody followed by FITC-labeled goat anti-mouse secondary staining (BD Biosciences) for surface HA expression. Cells were washed with PBS and fixed with 4% paraformaldehyde. Fixed cells were analyzed using FACSAria™ flowcytometer and MoFlow™ program.

Elispot. Blood samples were obtained from the Kraft Family Blood Donor Center or from volunteers under institute approved protocol. Elispot was performed using Ficoll-Paque purified Human PBMC's or red blood cell depleted mouse splenocytes (200,000 cells/well) co-incubated with the peptides (10μg/ml) or decreasing amounts in triplicate in Elispot plates (Millipore, Billerica, MA) for 18 h. Interferon-γ (IFNγ) secretion was detected using capture and detection antibodies as described (Mabtech AB, Nacka Strand, Sweden) and imaged using an ImmunoSpot Series Analyzer (Cellular Technology, Ltd, Cleveland, OH). Kb restricted OVA peptide, HLA-A*02:01 restricted Tax peptide and non-stimulated wells were used as negative controls. Spot numbers were normalized by removing the average back ground spot numbers calculated from negative control wells. CEF peptide pool that incorporates 32 EBV, CMV and influenza A was used as a positive control.

Mouse infection with influenza A/PR8/34 virus and mouse Elispot assays. Six to eight week old HLA-A02 transgenic AAD mice were anesthetized using 100mg/kg Ketamine and 15mg/kg Xylazine. Mice were infected with an intranasal sub-lethal dose of influenza/PR8/34 virus (Charles River Laboratories, Inc.). Time course of infection was followed by daily weight loss analysis. Three to four weeks post-infection, animals were euthanized and spleens were removed for Elispot analysis.

Cross-presentation assay. Human monocytes were isolated from HLA-A*02:01 positive donor PBMC's through plastic adherence. Dendritic cells were differentiated from adherent monocytes using GMCSF and IL-4 (100ng/ml Peprotech) supplemented complete DMEM media for one week. $A2^-$-BEAS were infected with influenza A/PR8/34 virus for 18 h. Infected dead floating cells were collected and plated in 6 well plates in 2 ml of OptiMEM media. Free influenza A virus in the dead floaters were inactivated using a UV exposure for 90 min using a hand held long wave UV lamp rested on the plates on a distance of approximately 0.5 cm from the surface of the fluid. UV inactivated floaters were plated with monocyte derived dendritic cells in 10:1 ratio in 24 well plates. Eighteen hours post incubation cells were harvested and HLA-A*02:01 on dendritic cells were immunoprecipitated for MS analysis. For cross-presentation assays involving SILAC, Dulbecco's Modified Eagle's Medium - low glucose deficient in L Arginine. L Lysine and L Leucine (Sigma D9443) was supplemented with 10% FBS (Sigma), L-glutamine (2 mM)(Gibco), penicillin (100 U/ml), streptomycin (100 μg/ml) (Sigma), 0.100 g/L L-Arginine-13C6, HCl (Pierce 88210), 0.100 g/L L-Leucine-13C6, (Pierce 88435), and 0.100 g/L L-Lysine-(Sigma L5501). LAZ 509 and 468 cells were cultured for over 10 generations in defined media in 37C° 5%CO2 incubator. Cells were infected with 10 EID_{50}/cell of IAV virus, UV inactivated as described and fed to monocyte-derived DC 10:1 ratio.

Detection of cytotoxicity, granular exocytosis by CD107A/B (LAMP-1/-2) staining. $M1_{58-66}$ specific T cell line was generated from an HLA-A02 positive donor previously identified to have a high frequency

influenza A $M1_{58-66}$ memory response. After two weekly of *in vitro* peptide stimulations, the resulting T cell line were used in the assay. $A2^+$-BEAS were plated at 50,000 cells per well in 96 well plates. Adherent $A2^+$-BEAS cells were infected with 10 EID_{50}/cell influenza A/PR8/34 virus for 18 h. Additional adherent $A2^+$-BEAS cells were loaded with decreasing concentrations of $M1_{58-66}$ peptide for one hour the day of the experiment. Wells were washed six times to remove unincorporated peptide or virus. $M1_{58-66}$ specific T cell lines were added in the wells in a 1:10 ratio. FITC-labeled CD107A and B antibodies (BD Biosciences) were added in the wells with the T cells. Cells were covered with aluminum foil and incubated at 37^{o}C in a humidified 5% CO2 incubator for 5 h. Cells were stained in the wells with $M1_{58-66}$ Dextramer (Immudex Denmark) for 30 minutes followed by CD8 alpha antibody (BD Biosciences) staining for 30 min. Cells were harvested, washed twice with PBS and fixed using 4% paraformaldehyde. Fixed cells were analyzed using FACSAria™ flowcytometer and MoFlow™ program.

Outline of Poisson Segmented LC-DIAMS method. Identification of immunologically relevant peptides presented as cell surface complexes with major histocompatibility class I (MHCI) proteins is a core technical challenge for developing vaccines to harness cellular immunity. For MS analyses, complexity, limited sample, and spectral crowding of doubly-charged molecular ions in the m/z range 450-600 challenge a focus limited to a very few specific peptides that mark the cell as infected or transformed. T cells can recognize a very few (3) copies of a peptide displayed by a cell; MS identification is challenged to do as well. For vaccine development identifying an ocean of normal 'self' peptides is irrelevant. Conventional data-dependent acquisition (DDA) MS identifies ions largely in order of their intensity. Where samples are complex, DDA MS does not plow deep enough through the 'self' peptides to uncover the interesting (e.g., foreign) peptides. Here we apply a data-independent acquisition (DIA) format with Poisson detection (Poisson LC-DIAMS). This format allows collected MS data to be analyzed for targets (e.g., immunologically relevant peptides) defined post-acquisition. We have implemented three components necessary for high performance detection. The first concerns liquid chromatography. We have employed ultra low flow LC (10 nl/min) using a 2 cm segment of a 50 um ID capillary with C10-modified polystyrene-divinylbenzene monolithic bed(4) as a precolumn and a 15 cm, 20 um ID capillary with a C18-modified polystyrene-divinylbenzene monolithic bed as an analytical column. The second component concerns optimal data acquisition on a pulsed extraction quadrupole-TOF. Band transmission for DIA is a simple matter of changing the resolution parameters for the quadrupole. For MHCI analyses, 30 m/z-wide selection windows are used to cover the range m/z 440 - 620. The transmission bands are not placed side by side as in SWATH collection but overlap by half. This requires monitoring 11 instead of 6 bands but by taking linear combinations of these bands one can effectively restrict precursors into 15 m/z-wide windows with the same number of ion events as if six 30 m/z-wide non-overlapping bands were collected in the same period. The high energy fragmentation spectra are also acquired using the pulsed extraction feature proprietary to ABSciex quadrupole-TOF instruments. Pulsing is tuned to improve the sensitivity over the m/z range from 550-1000, the most important for diagnostic fragments of doubly-charged MHCI peptides. The third component is Poisson detection. This uses the same formal structure of sampling a Poisson process as MS^3 detection (5) except the amplitude of embedding a reference pattern is plotted as a function of scan number, i.e., one constructs a Poisson chromatogram.

Figure **S1** is an example of a XIC/Poisson chromatogram for detecting a target in an LC-DIAMS dataset. The black trace on top is the extracted ion chromatogram (XIC) for the precursor ion plotted as a function of scan number (elution time) while the inverted blue trace is the Poisson chromatogram for the target ion's fragmentation pattern. The pattern could be from a library of fragmentation spectra or it could be directly measured with a synthetic peptide analog on the same instrument used for the LC-DIAMS sample run. We have used primarily the latter approach. The positive y scale in Figure **S1** is ion counts, that is, this instrument has a point detector and measures individual ion arrival events. The Poisson chromatogram also has dimensions of ion events and is proportional to the precursor ion amplitude but the factor is related to the fragmentation pattern. **For the descending Poisson chromatogram a scale is chosen so that in the reference LC-DIAMS run that acquired the fragmentation pattern the Poisson peak has the same magnitude as the XIC peak.** That is, if the LC-DIAMS run of the synthetic peptide had an XIC peak of 100 ion events and a corresponding Poisson peak of 50 ion events a scale factor of 2 would be applied to the Poisson chromatogram for this peptide in any future run. Reflecting sample complexity, both the XIC and Poisson traces in Fig. **S1** have multiple peaks but at the elution position of the target one expects both a peak in the XIC as the precursor ion appears and a coincident peak in the Poisson chromatogram as the target fragmentation pattern in the band MS^2 spectra also appears. The coincidence is marked with an arrow in Fig. **S1**. Both the XIC and Poisson chromatograms are first Fourier transformed, then weighted in Fourier space to remove both baseline features (low frequencies) and shot noise (high frequencies), and finally inverse Fourier transformed (6).

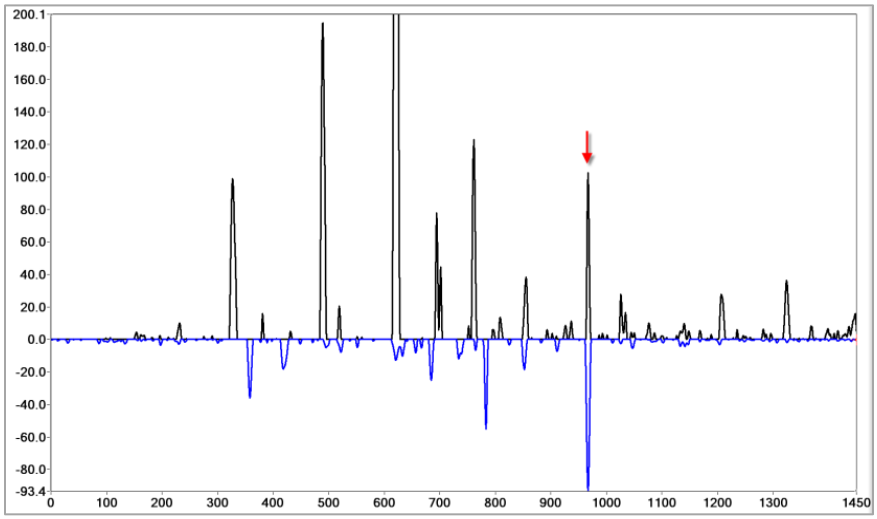

Figure S1. Detection chromatogram identifies coincidence of precursor ion and fragmentation pattern as a function of LC elution position in scan number.

For target detection one also requires the scan position of the XIC/Poisson coincidence to be consistent with the measured elution behavior of the synthetic peptide relative to endogenous peptides. For this, LC-DIAMS data for elution mapping is independently acquired in which synthetic peptides are added to an extract of endogenous MHCI peptides. These endogenous peptides are also found in the sample being analyzed for target peptides. Then paired scan positions (i.e., reference, experiment pairs) of endogenous peptides and targets from both LC-DIAMS runs are plotted. All scan pairs should fall on a single elution line (see Fig. 1D of manuscript).

Quantitation of IAV Peptides as Copies/Infected Cell. BEAS cells were infected with IAV strain A/X-31 and the peptide-HLA-A2 complexes affinity immobilized on beads (see Methods). The beads were washed, suspended in water and split into equal parts by volume, maintaining the suspension. 500 attomoles of isotope labeled **GIL^{h}GFVFTL** was added to one part (1.67 million cells) and this sample was analyzed by segmented LC-DIAMS (Identified in the following as h14_94 sample run. Poisson detection plots for the IAV peptides from the X-31 sample are shown in Figs. S5). In the manuscript (Fig. 3D) the quantitation of the **GILGFVFTL** peptide from the ratio of XIC peaks areas with the added 500 attomoles of **GIL^{h}GFVFTL** is illustrated. The method is straightforward but isotope-labeled peptides are expensive. The combination of interest in the immunodominant response to $M1_{58\text{-}66}$, its extreme hydophobicity and the observed losses and ion suppression with this peptide warranted the expense. For the other IAV epitopes we used a less expensive alternative in which a mixture of 500 attomoles of synthetic peptides with natural isotopic composition was added to an equivalent aliquot of the infected BEAS sample. This was also analyzed by segmented LC-DIAMS (Identified in the following as sample run h14_95). The manuscript examined quantitation of the $PB2_{463\text{-}471}$ peptide based on relative peak areas of the extracted precursor ion chromatograms; here we extend quantitation in the infected sample to other peptides. Figure **S2** shows XIC 467.257 chromatograms for NMLSTVLGV from the two LC-DIAMS runs. In order to measure the integral the precursor ion intensity must be large enough over the ion background. In the top panel of Fig. **S2** the ion background is about 20 events with a peak of 90 events. The inscribed box shows the integrated region. One cannot immediately take the peak area ratio of the two sample runs as ion flux into the mass spectrometer depends on factors external to the sample which are difficult to control on nanoscales. Since the two LC-DIAMS runs are of equal aliquots precursor ion amplitudes of a set of endogenous peptides can be used to normalize the intensity between the two runs (h14_94 and h14_95). NMLSTVLGV elutes at scan 1200 with the amplitude ratio h14_94/h14_95 for endogenous peptides here being roughly 1.8 so the 450 area becomes 450/1.8 = 250. That means the 15,330 area in h14_95 consists of 500 attomoles of added NMLSTVLGV plus 250 from infection. 500 attomoles of NMLSTVLGV then generates a peak area of 15,080 and 250/15,080 x 500 = 8 attomoles from infection of 1.67 million cells. Translated into copies per cell (8 x 6 x 10^{5}/1.67x10^{6}), we find roughly 3 copies per cell.

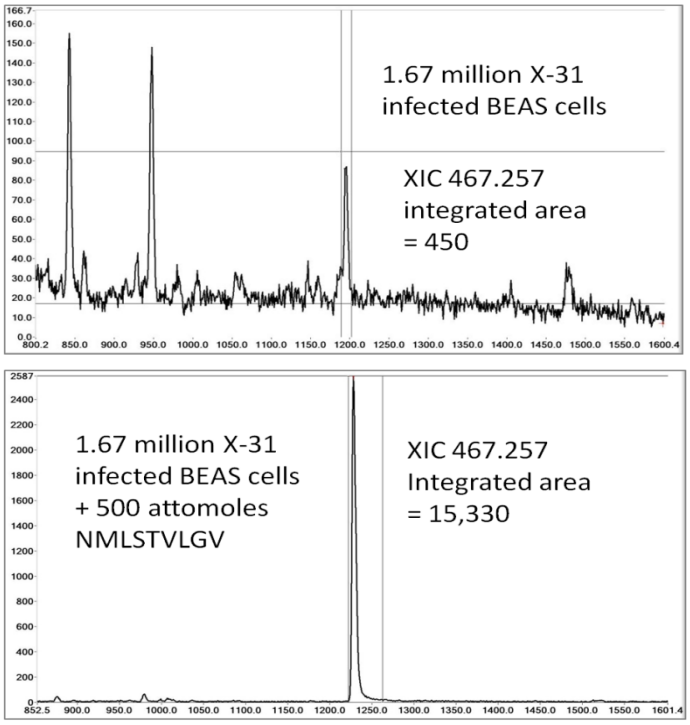

Figure S2. XIC peak areas for elution of NMLSTVLGV from infected sample and infected sample with 500 amols of added synthetic peptide.

Consider the same exercise for $M1_{134-142}$ RMGAVTTEV. **Fig. S3** shows XIC 482.25 plots with peak areas. The normalization factor between h14_94 and h14_95 is 4 around scan 200 so 11000/4 = 2750 would be the contribution of the infection to the integrated RMGAVTTEV signal in h14_95. To get just the signal from 500 amols in h14_95, the infection contribution must be subtracted, giving an integrated XIC signal of (6978-2750 =) 4228. Then 2750/4228 * 500 = 325 amols in the infected BEAS sample. 325 amols/1.67 * 10^6 = 32.5 * 6 / 1.67 = 117 copies/cell of RMGAVTTEV.

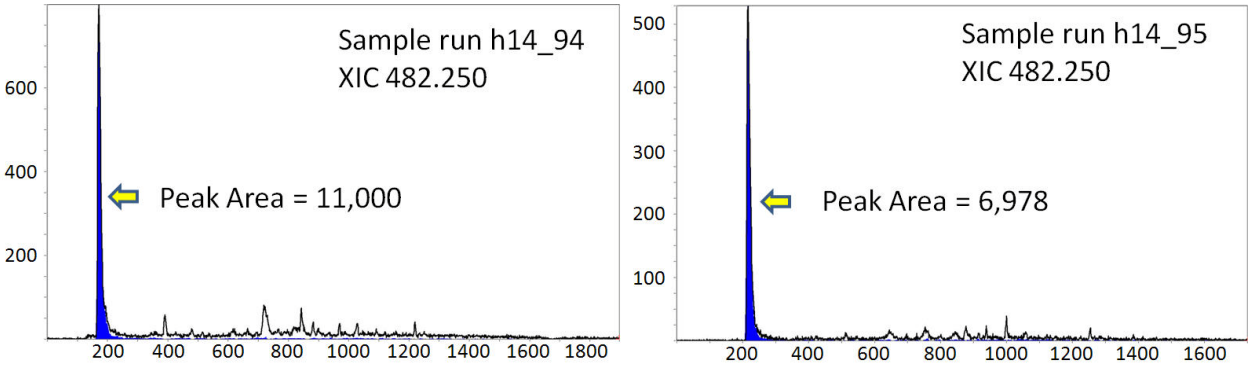

Figure S3. Peak areas for RMGAVTTEV in infected sample (h14_94) and infected sample with 500 amols of added synthetic peptide (h14_95). Peak areas must be normalized for signal response between the two runs.

The $M1_{3-11}$ peptide **LLTEVETYV** is quite sensitively detected with 500 attomoles added sample (h14_95) producing a peak area of 46,500 ion events while the infection only gives 250 ion events (Fig. **S4**, inset showing integration detail). At scan 1000 the amplitude normalization factor is 2 and putting these together, 125/46413* 500 = 1.3 amols from infection or 0.47 copies/cell.

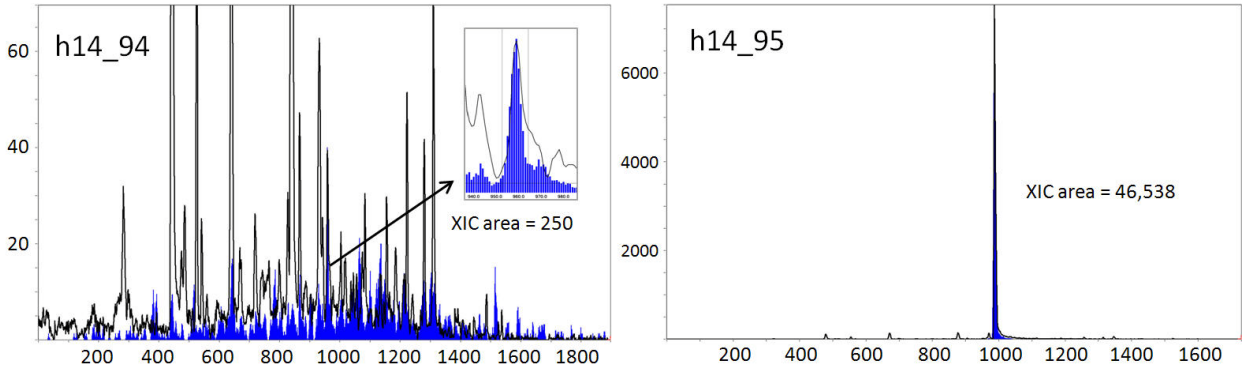

Figure S4. Peak areas for LLTEVETYV in infected sample (h14_94) and infected sample with 500 amols of added synthetic peptide (h14_95).

The quantitation of the $M1_{58-66}$ peptide **GILGFVFTL** provides a significantly different situation from **LLTEVETYV**. At scan 1650 the intensity normalization factor for the two runs is 1. Then 201 of the 273

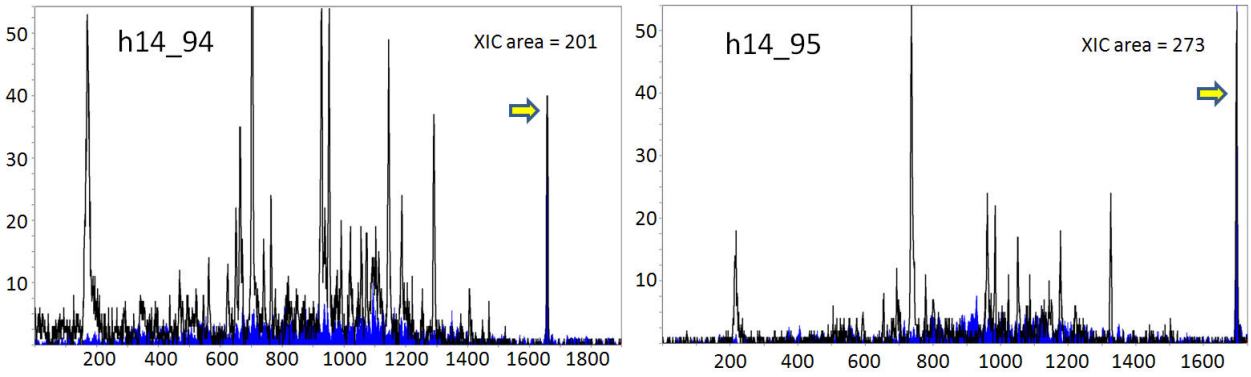

Figure S5. Peak areas for GILGFVFTL in infected sample (h14_94) and infected sample with 500 amols of added synthetic peptide (h14_95).

integrated events in h14_95 are coming from infection and only 72 are from the added 500 amols (Fig. **S5**). Calculated as before, one has 201/72 * 500 amols = 1395 amols from infection, or 501 copies/cell. In Fig. 3D of the manuscript the copy number per cell of $M1_{58-66}$ is also calculated relative to 500 amols of added isotope-labeled **GIL^{h}GFVFTL** peptide in h14_94, giving roughly 1000 copies/cell. **GIL^{h}GFVFTL** (500 attomoles) was also added to h14_95 (Fig. **S6**). Here 50 ion events as the integrated signal of 500 amols of labeled $M1_{58-66}$ peptide in h14_95, light or heavy, one has 273 = 223 + 50 (infection + 500 amols added light $M1_{58-66}$ peptide) or 223/50 * 500 amols = 2230 amols from infection or 645 copies/cell.

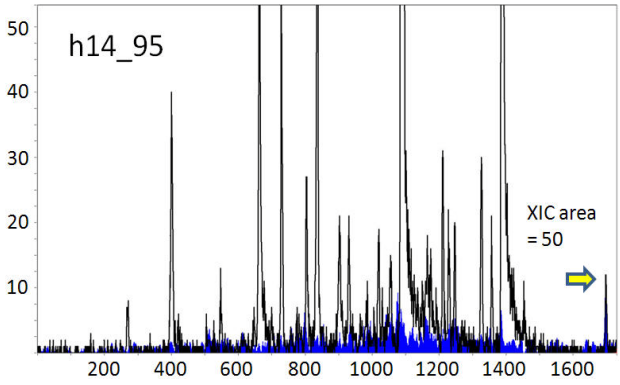

Figure S6. Peak area for isotope-labeled peptide GIL^{h}GFVFTL in h14_95.

MS^3 quantitation of $M1_{58-66}$ Given the isotopic analog of the $M1_{58-66}$ peptide it is also possible to quantitate the peptide in infected cell A2 peptide isolates by static nanospray MS^3. For this method one first determines the ratio of Poisson MS^3 event counts at fixed cutoff probability (5) for an equimolar mixture of synthetic labeled and unlabeled forms. The mixture is run by static nanospray on a QTrap 4000 using an acquisition sequence that alternated between transitions for the heavy analog and the light analog. We measured 0.8 for the Poisson count ratio of light to heavy forms. Note there is no expectation of equivalence here as fragmentation by vibrational dissociation explicitly involves mass dependent nuclear motion. To detect GILGFVFTL in IAV infected cells, 5 fmols of the heavy analog (GIL^{h}GFVFTL) was added to an A2 extract of peptides from 1.67 million A/Victoria/3/1975 infected BEAS cells and the mixture was analyzed by nanospray MS^3 for both the light and heavy forms using the same acquisition sequence. Poisson detection plots gave a ratio of 62/103 x 0.8 x 5 fmols = 2.4 fmols of GILGFVFTL from infection (**Fig. S7**). 2.4 x 6 x 10^8 molecules/1.67 x 10^6 cells = 860 copies/cell of $M1_{58-66}$ from infection.

Quantitation on small sample scales is generally a challenge. This is more of an issue where the analyses are not running a small aliquot of a concentrated sample. Rather, sample preparation for each run involves substantial handling: acid elution of peptides from affinity immobilized pMHCI complexes, C18

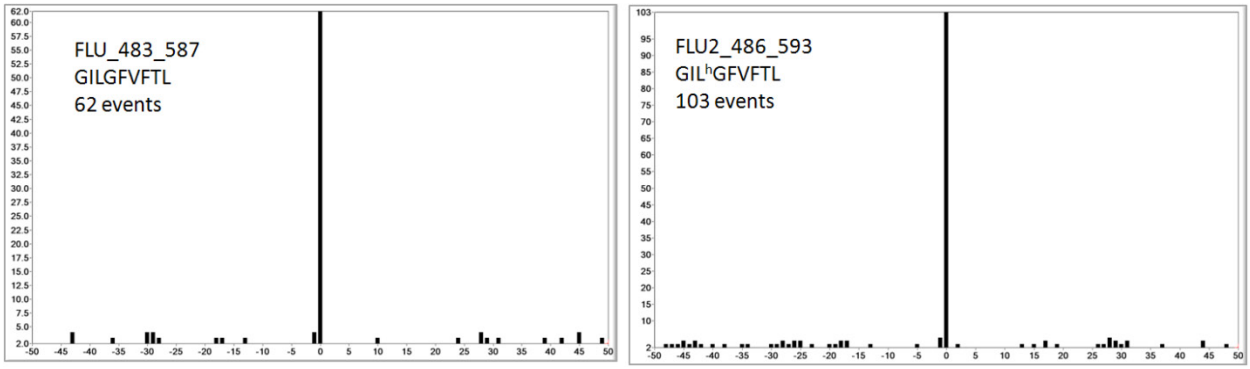

Figure S7. MS^3 Poisson detection amplitudes for unlabeled and isotope-labeled GILGFVFTL in an IAV Victoria/3/1975 infected BEAS sample with 5 fm of added isotope-labeled GIL^{h}GFVFTL.

phase extraction, washing, elution, volume reduction, and sample loading for nanospray or LC-MS. Therefore we have applied different approaches using LC-DIAMS and a very orthogonal MS^3 method to show that the M1$_{58\text{-}66}$ peptide GILGFVFTL is abundantly presented in IAV infection with copies/cell in the range of 500-1000.

For the NS1$_{122\text{-}130}$ peptide **AIMDKNIIL** we did not have a synthetic version, either crude or pure, for quantitation. Normalized to the 500 amols of M1$_{3\text{-}11}$ peptide **LLTEVETYV** added in h14_95 (**Fig. S8**), the ratio of XIC peak areas 5220/46538 would give roughly 20 NS1$_{122\text{-}130}$ copies/cell. Other purified synthetic influenza peptides that elute in the middle of the chromatogram give peak areas relative to **LLTEVETYV** decreased by factors of 2 or 3. This would increase the **AIMDKNIIL** copy number accordingly, so that a rough range is 20 to 60 copies per cell.

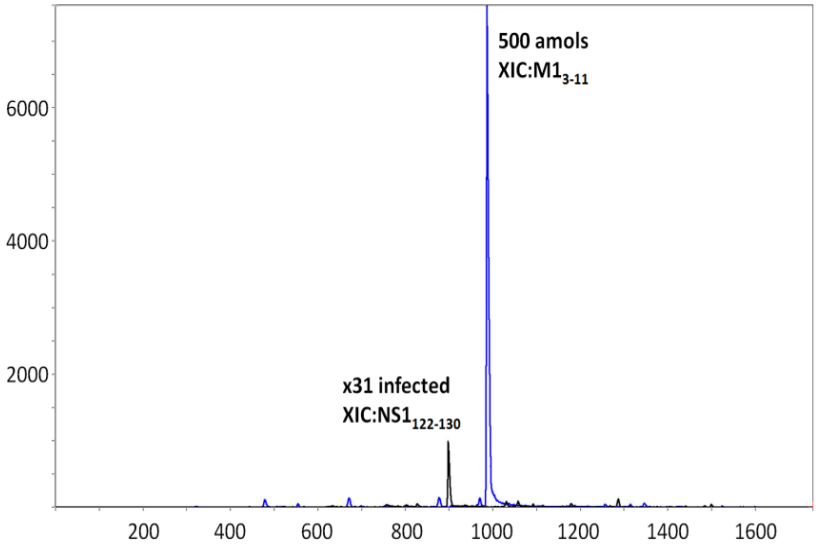

Figure S8. XIC peak areas of AIMDKNIIL (from infection) and LLTEVETYV (overwhelmingly from adding 500 attomoles of synthetic peptide) in h14_95 sample.

Figure S9. Poisson MS^3 detection plots. MS^3 spectra of transitions for target peptides acquired from infected and naive BEAS cells are compared by a Poisson metric against reference MS^3 spectra experimentally generated from synthetic peptides. Target detection is associated with a dominating '0-translation' peak (5) compared with naive samples. The analysis is done by static nanospray ionization without chromatographic separation of peptides and uses MS^3 spectra. Sample amounts are a few million BEAS cells, the same sample scale as the 10 nl/min LC-DIAMS analyses shown in Fig S2. Neither MS^3 nor LC-DIAMS is optimal for detecting all IAV peptides; poor fragmentation patterns limit MS^3 while ionization suppression and surface adsorption limits LC-DIAMS.

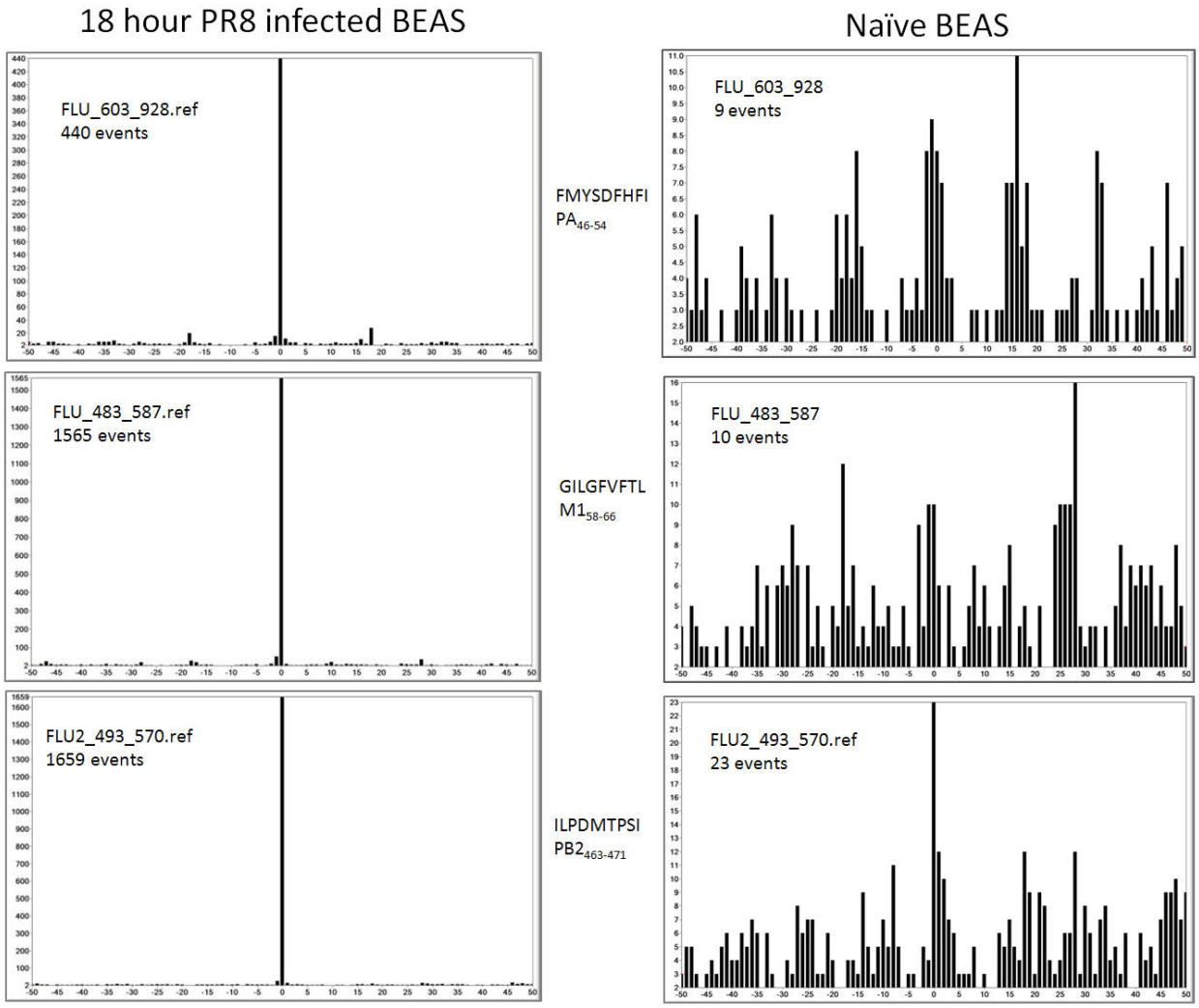

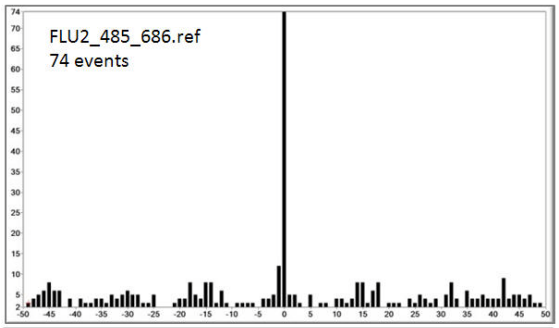

GLISLILQI
NA_{18-26}

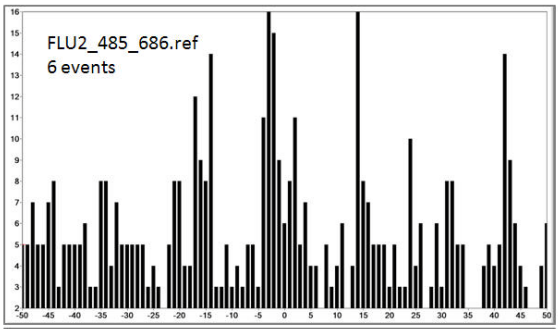

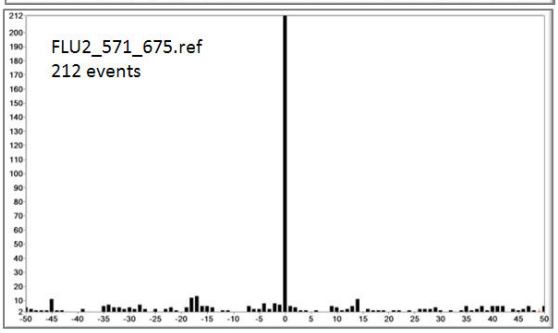

FLDIWTYNA
$HA_{431-439}$

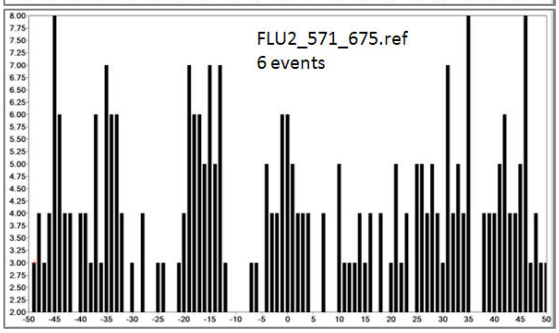

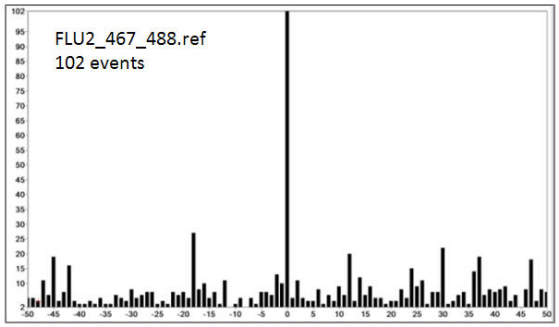

NMLSTVLGV
$PB1_{413-421}$

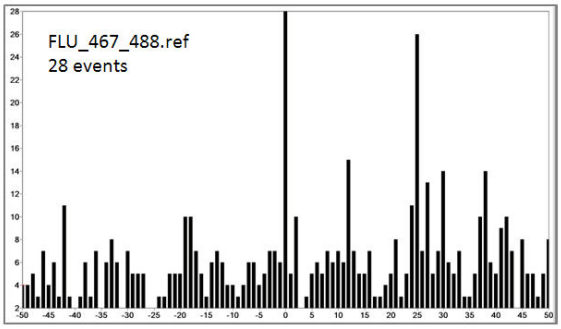

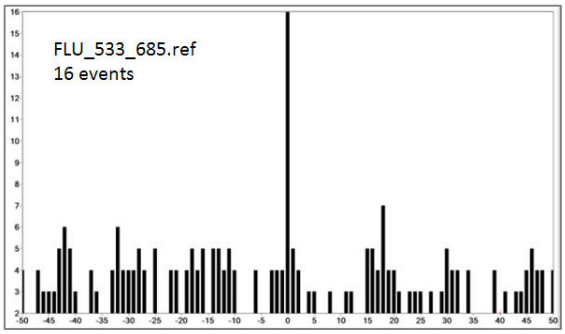

LLTEVETYV
$M1_{3-11}$

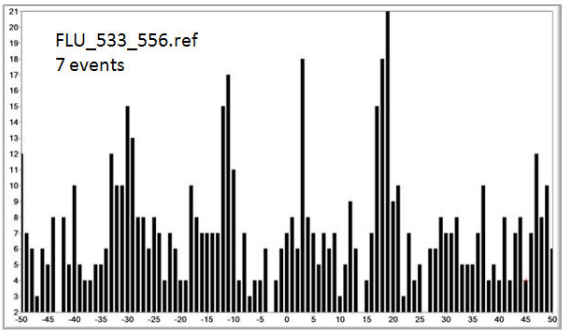

Figures S10. Poisson segmented LC-DIAMS detection of HLA-A02:01 bound IAV peptides in 18 hour infection by IAV strain A/Puerto Rico/8/1934 (PR8) of a sample of 5 million BEAS-2B cells, a bronchial airway epithelial cell line transfected with HLA-A02:01. Extracted ion chromatograms (XICs, trace in black) and Poisson chromatograms (bottom, negative orientation, trace in blue) for 8 identified IAV peptides are shown. For each of these peptides, analogs had been synthesized for fragmentation patterns and elution positions relative to endogenous HLA-A02 marker peptides. The peptide (and protein source in a reference PR8 proteome) whose fragmentation pattern is used in the Poisson detection is shown above the plot. In these plots the horizontal (x) units are scan number (dimensions of time) and vertical (y) units are ion counts in the positive direction and scaled ion counts at a cut-off probability in the negative direction. The scale parameter is derived from the XIC/Poisson ratio of the synthetic peptide. A brief description of the detection chromatogram is given in the section ***Outline of Poisson LC-DIAMS method*** with the mathematical description in application to MS^3 detection published (5). The detection position in the chromatograms associated with co-incident XIC and Poisson peaks are marked with an arrow.

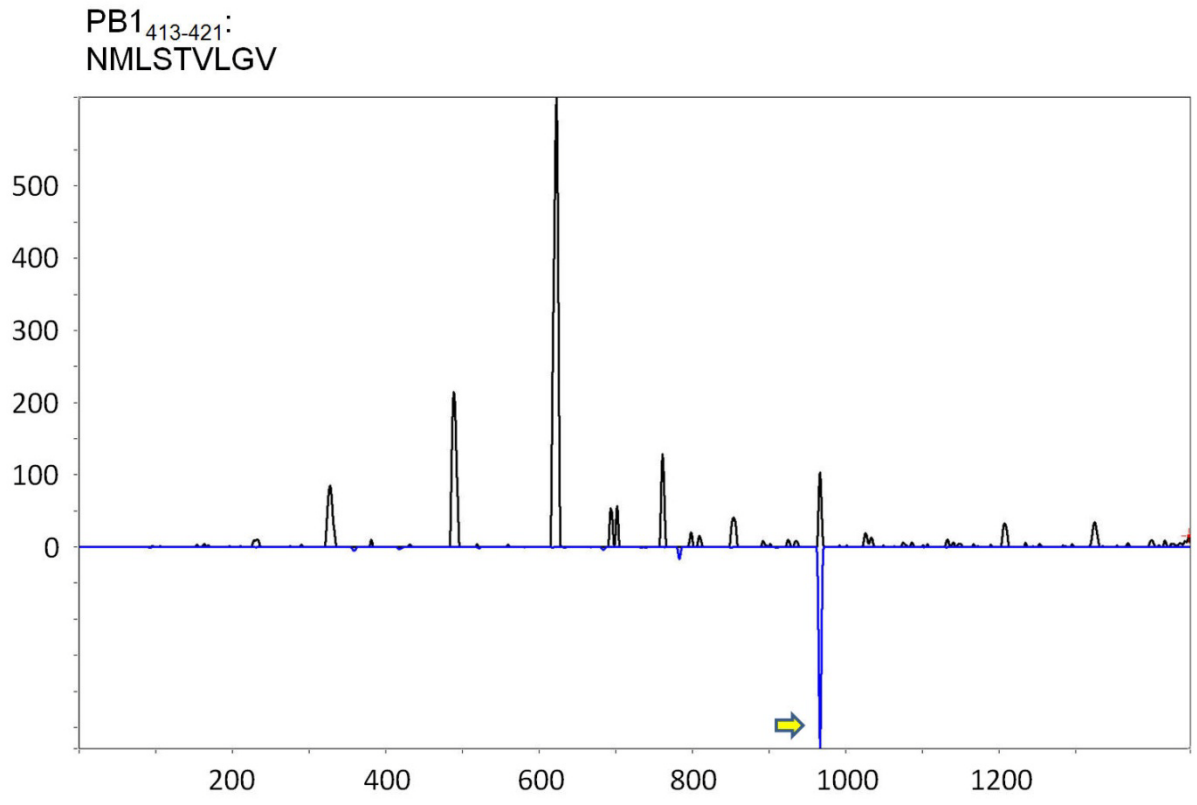

$M1_{134-142}$:
RMGAVTTEV

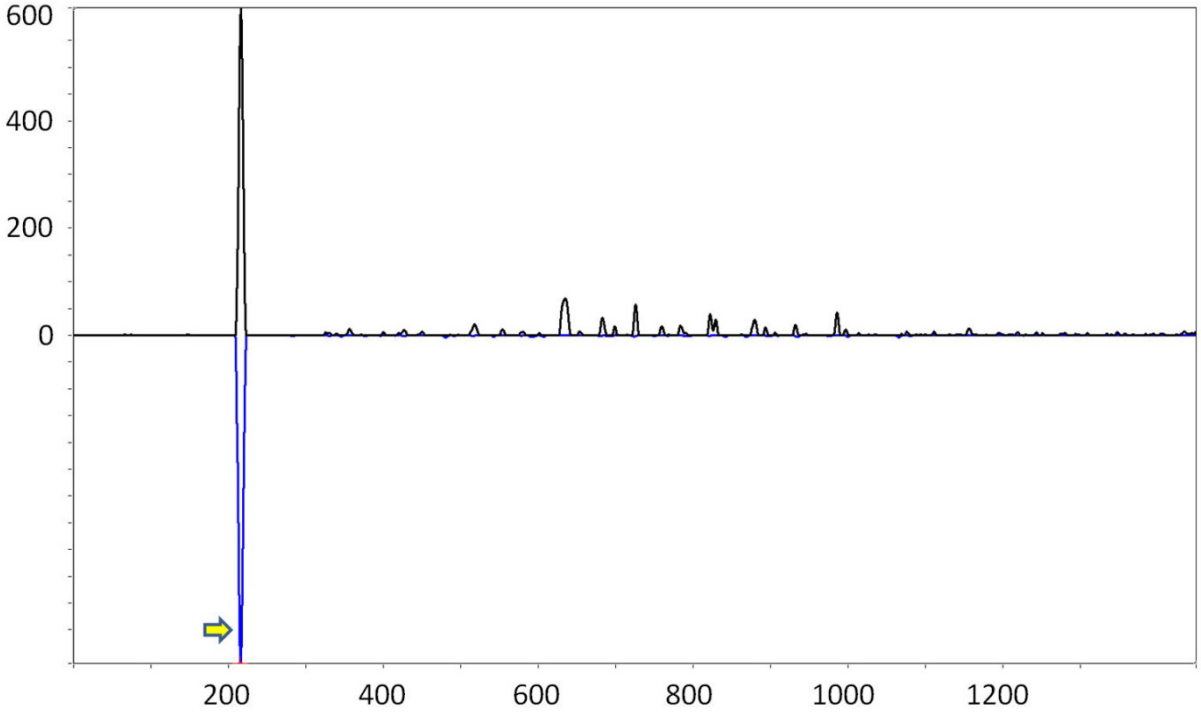

$M1_{58-66}$:
GILGFVFTL

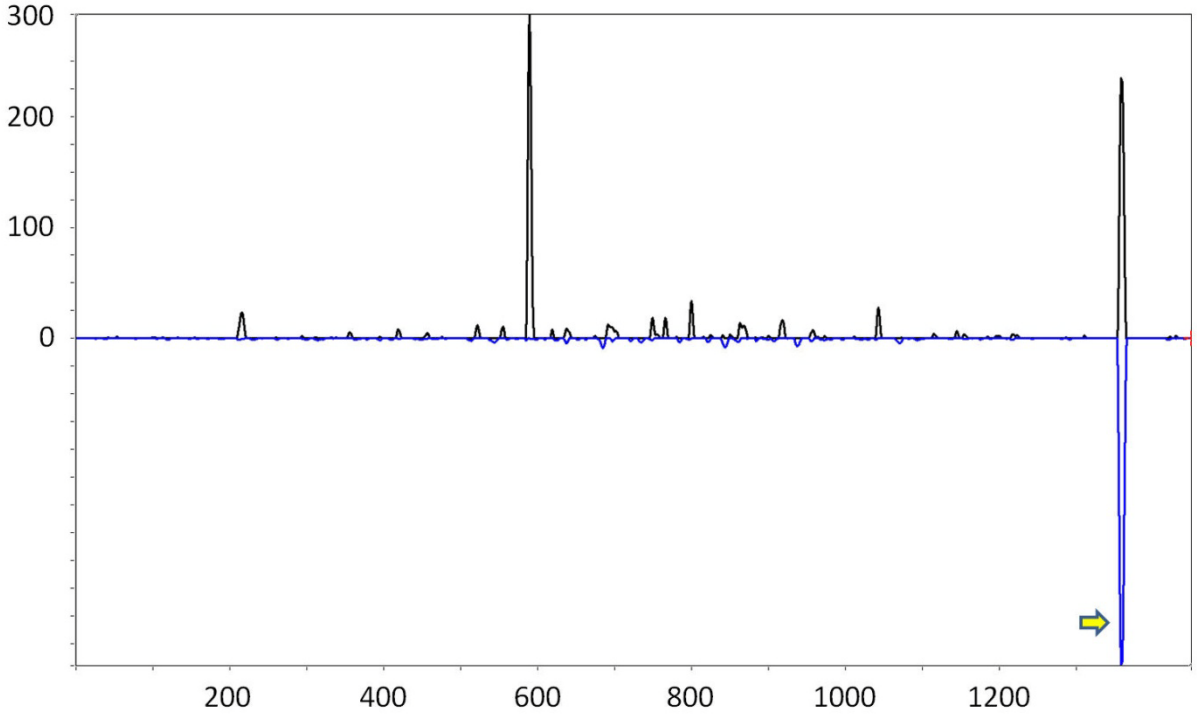

NA_{18-26}:
GLISLILQI

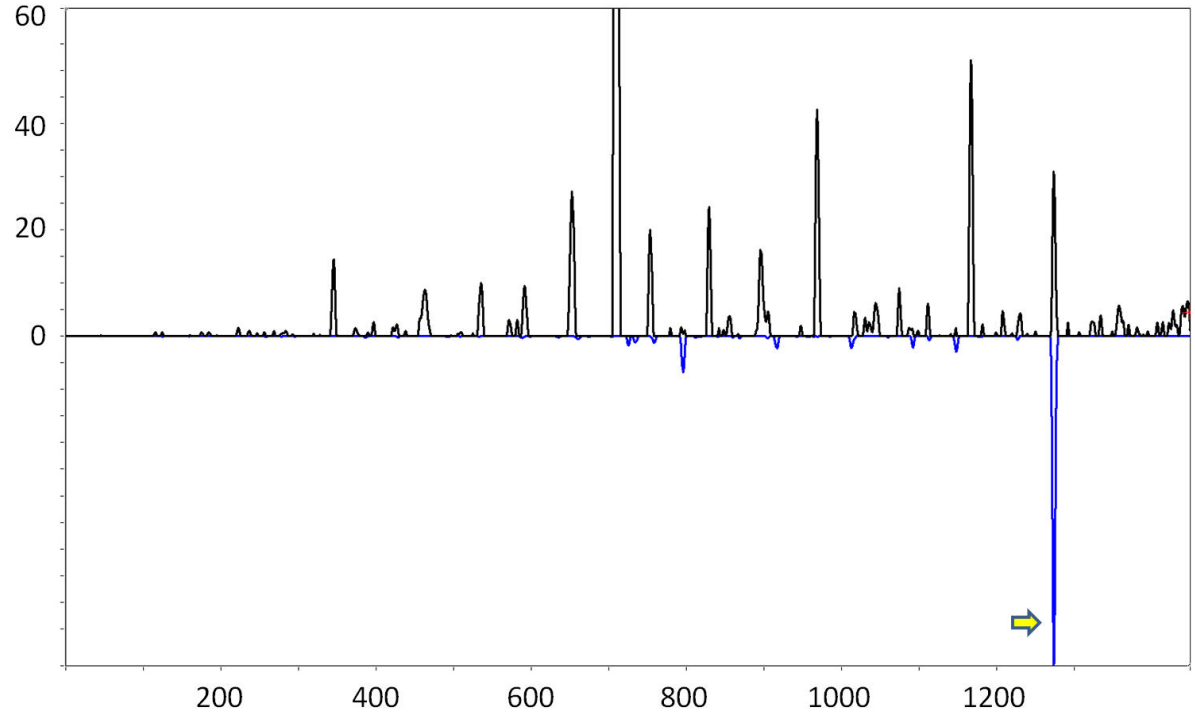

$PB2_{463-471}$:
ILPDMTPSI

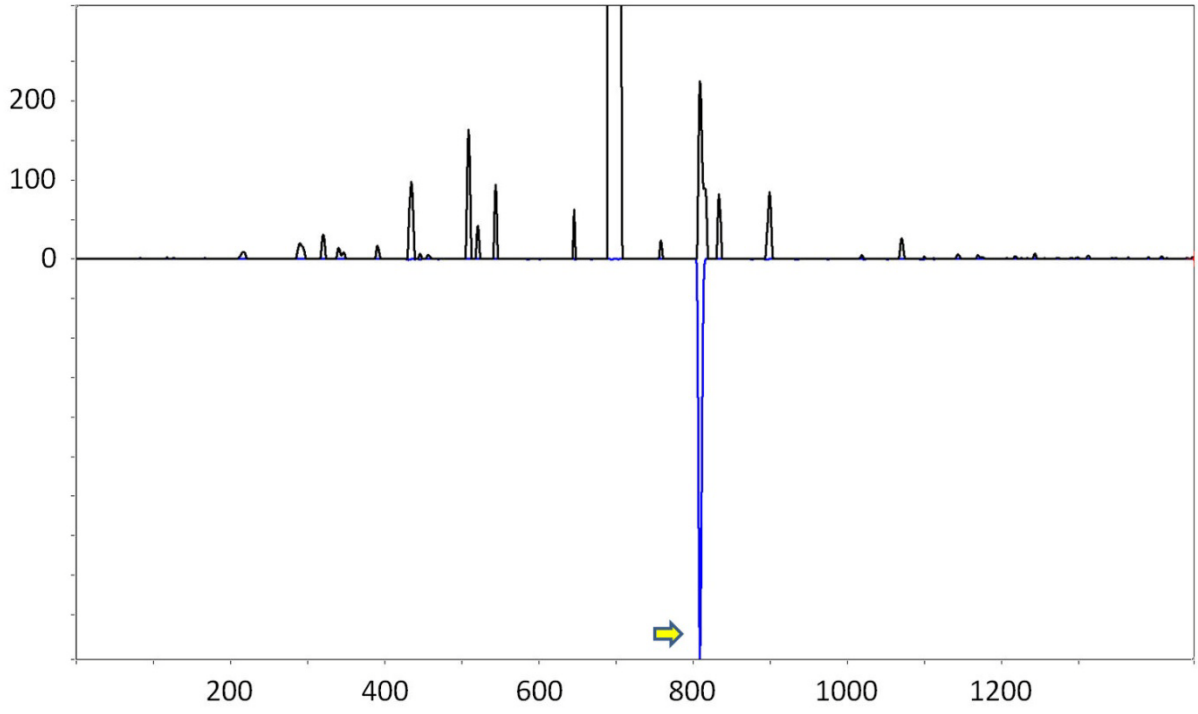

$M1_{3-11}$:
LLTEVETYV

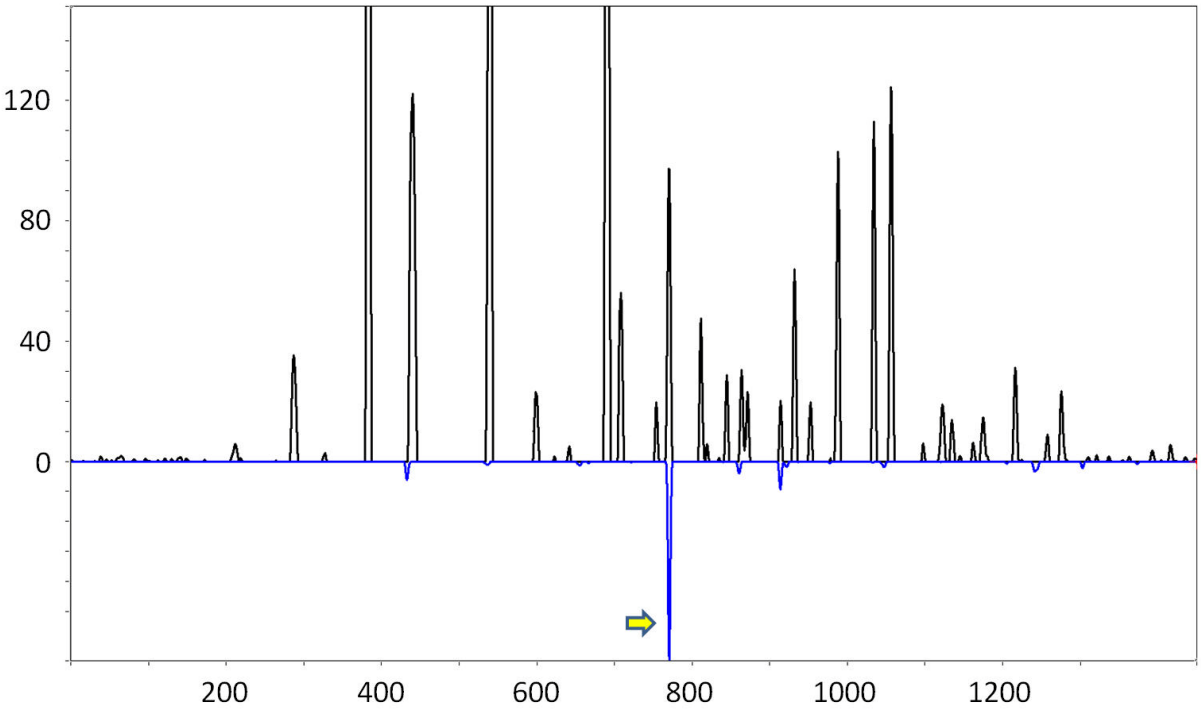

$HA_{431-439}$:
FLDIWTYNA

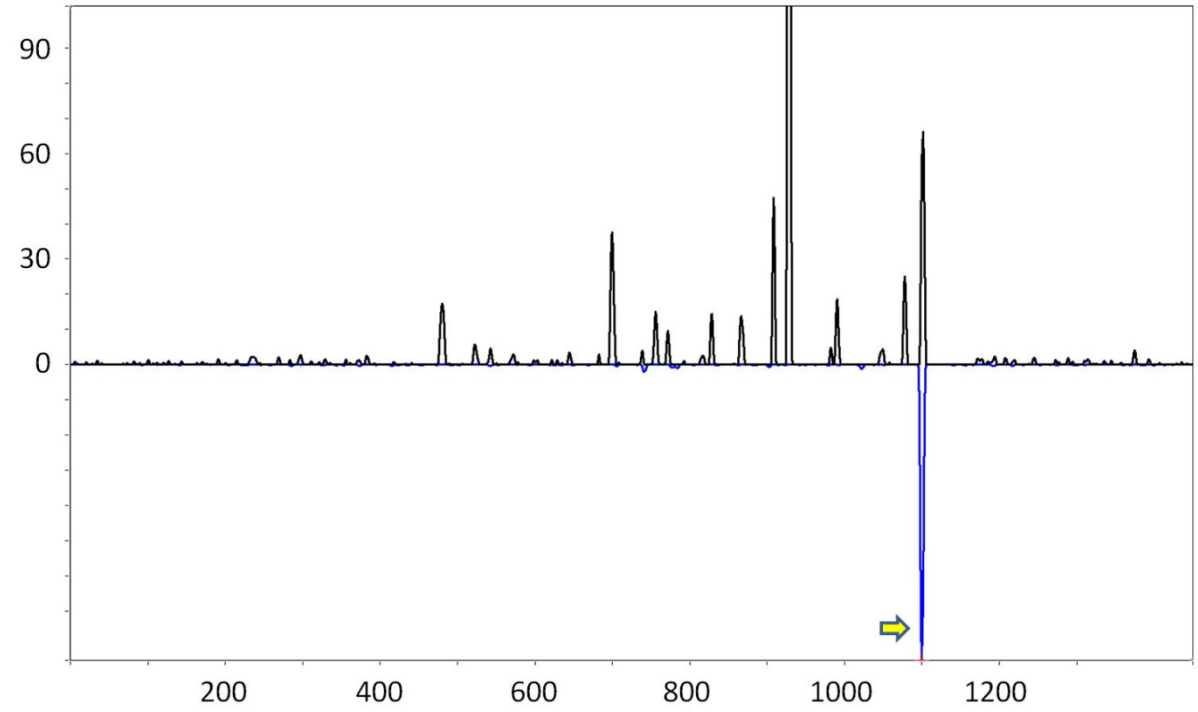

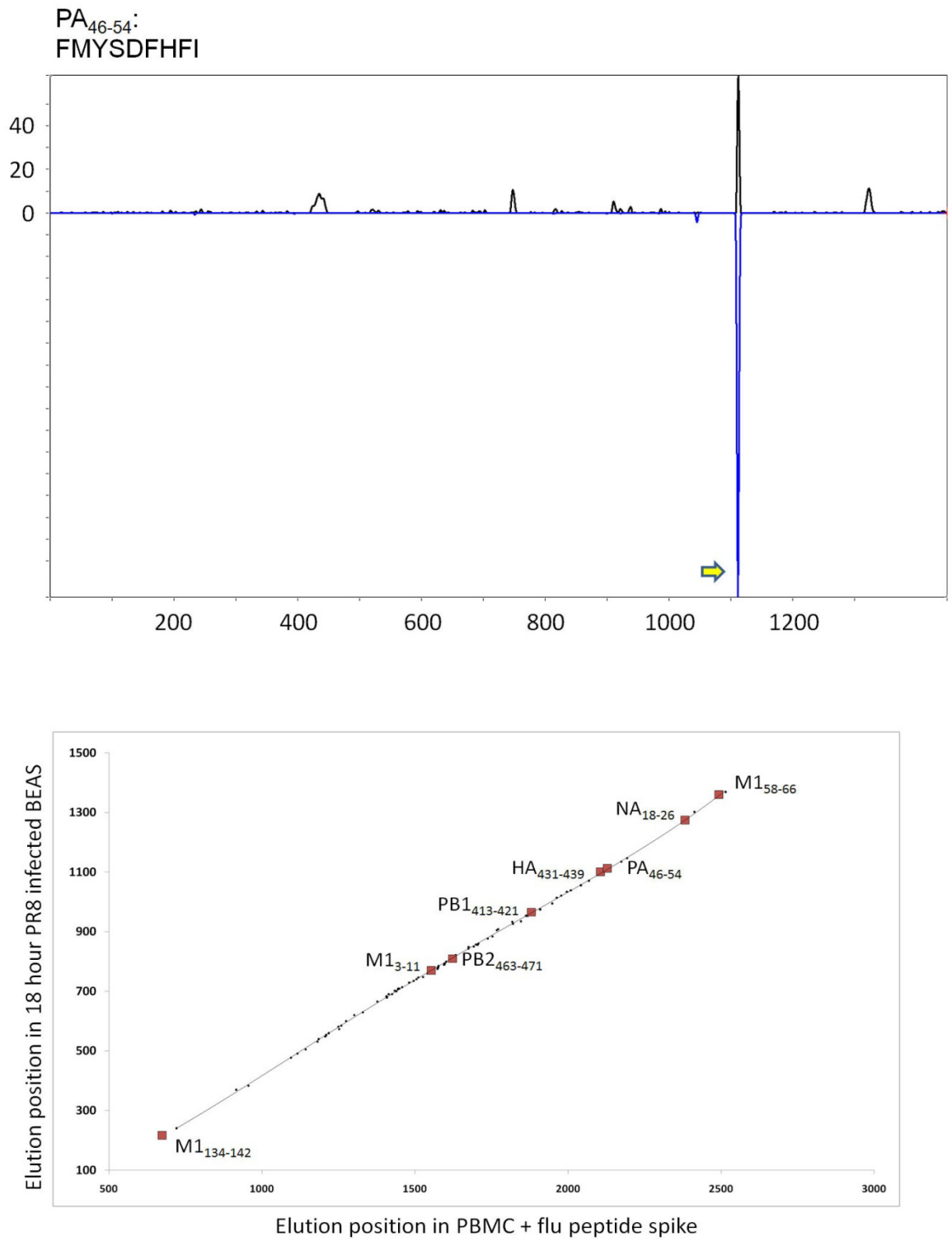

Fig. S10a, above. Elution plot of shared endogenous peptides showing detected positions of IAV peptides. All points are (x, y) = (scan position in PBMC spike, scan position in infected BEAS). The solid line is a low order polynomial fit to endogenous peptide position pairs.

Figure S11. Negative detection of 23 synthesized peptides in 18 hour PR8 infection of BEAS cells. These chromatograms are generated from the same LC-DIAMS data that gave positive detection of eight PR8 peptides in Fig. S2 above. The detection plots are of the same character as Fig. S2 with the predicted elution position of the IAV peptide in the infected BEAS sample marked with an arrow. This position is calculated from the elution position of the peptide in the PBMC spike-in sample and the polynomial fit to the elution line (Fig. S2a above).

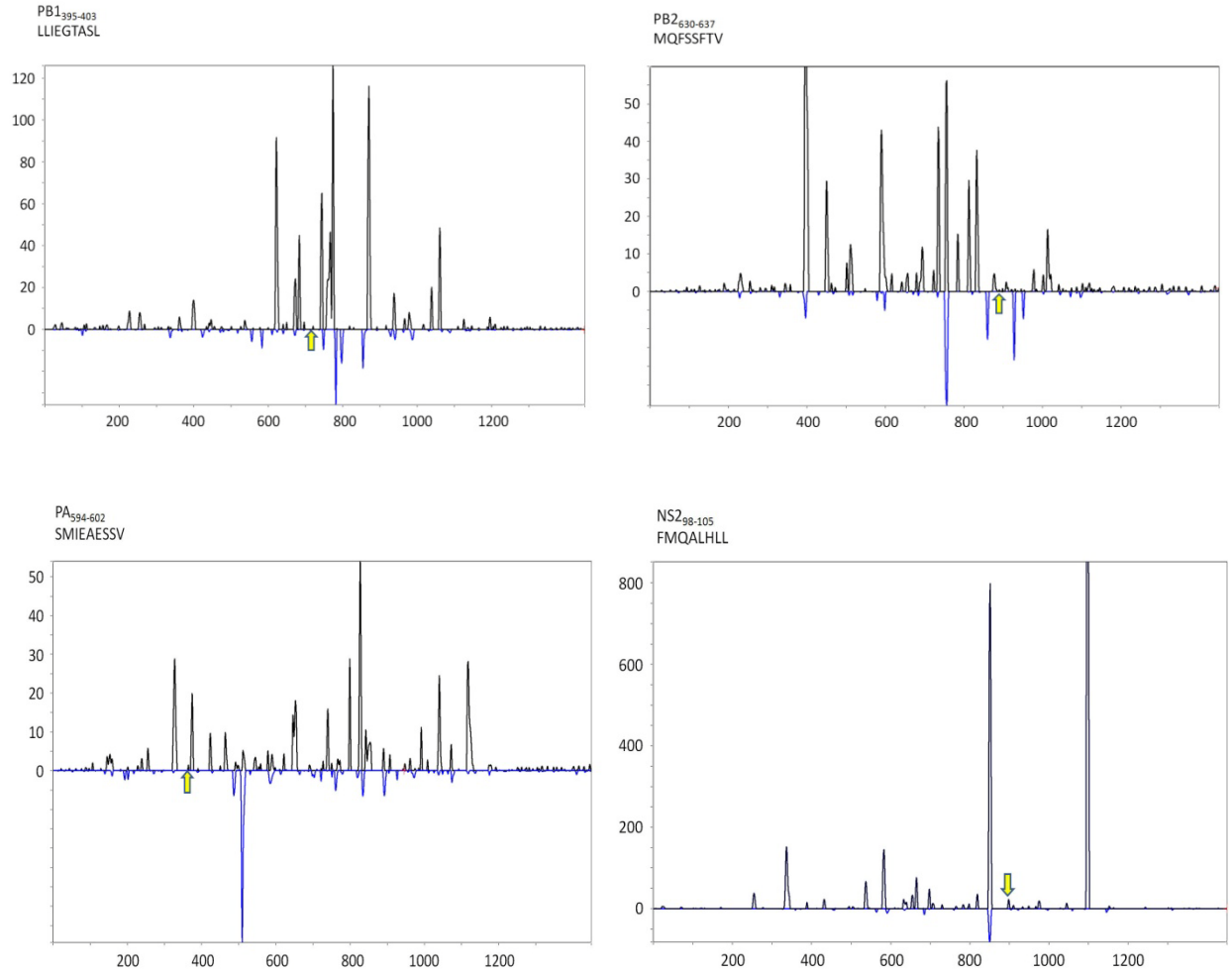

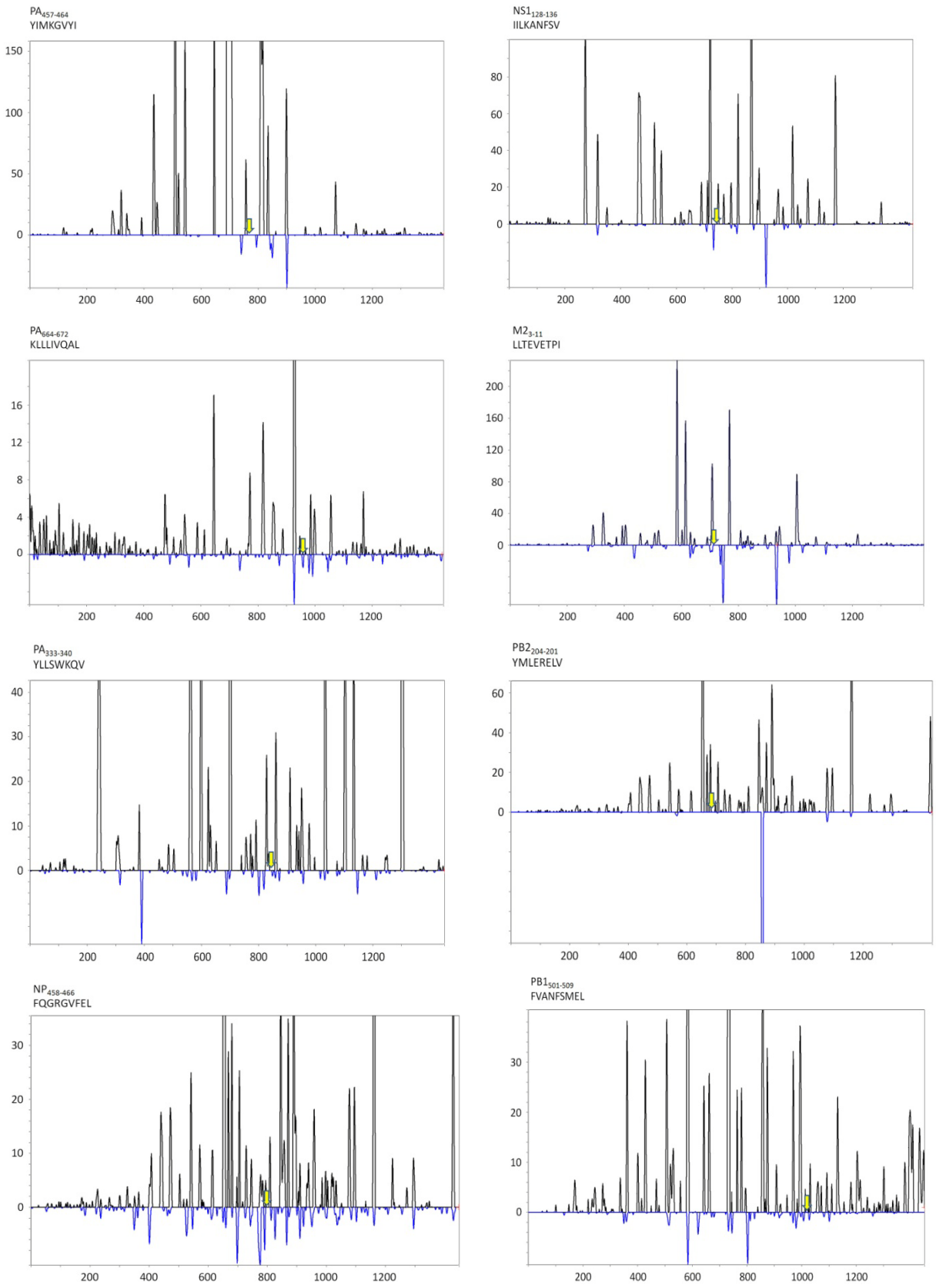
PA457-464
YIMKGVYI
NS1128-136
IILKANFSV
PA664-672
KLLLIVQAL
M23-11
LLTEVETPI
PA333-340
YLLSWKQV
PB2204-201
YMLERELV
NP458-466
FQGRGVFEL
PB1501-509
FVANFSMEL

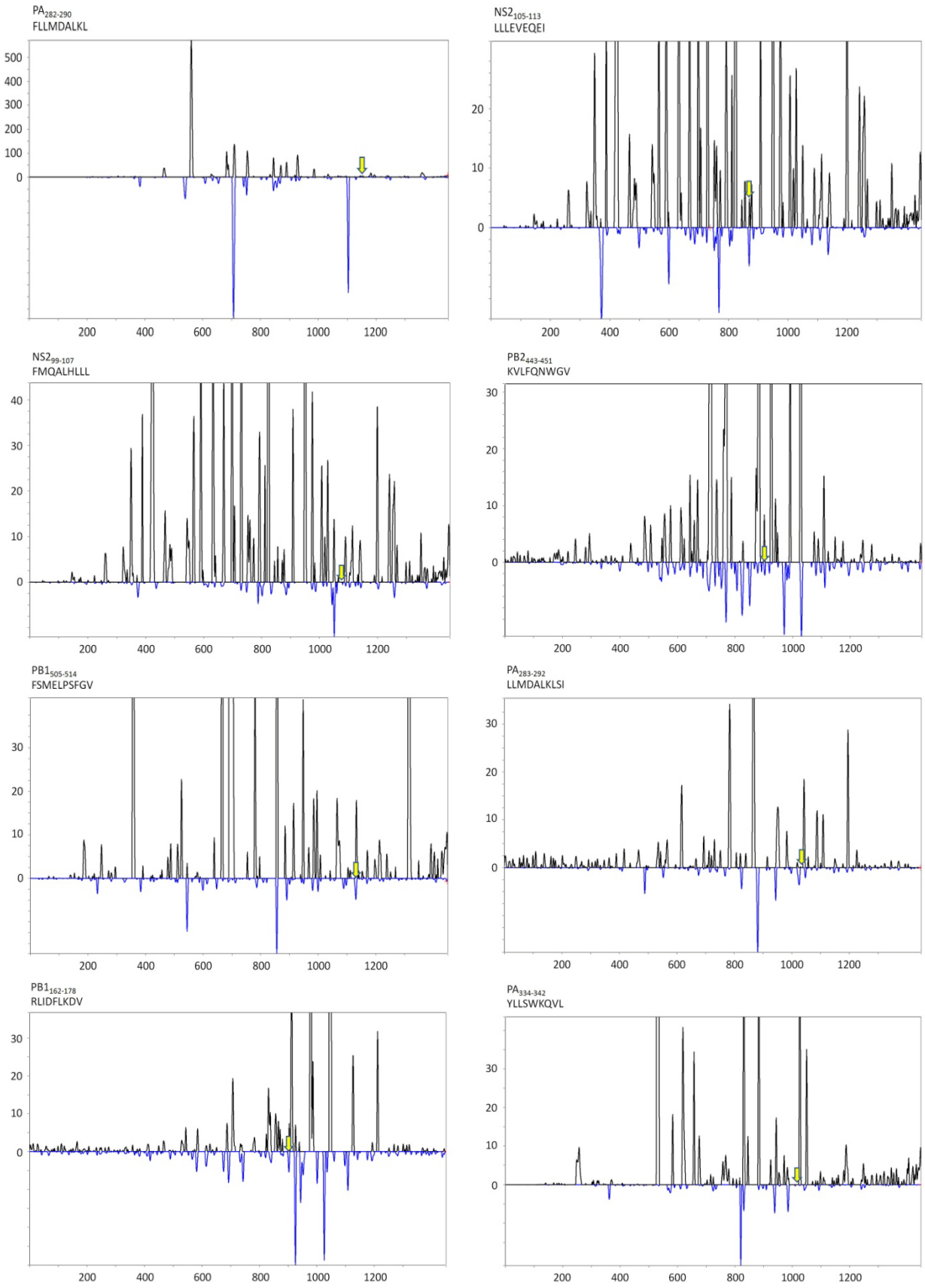
PA282-290
FLLMDALKL
NS2105-113
LLLEVEQEI
NS299-107
FMQALHLLL
PB2443-451
KVLFQNWGV
PB1505-514
FSMELPSFGV
PA283-292
LLMDALKLSI
PB1162-178
RLIDFLKDV
PA334-342
YLLSWKQVL

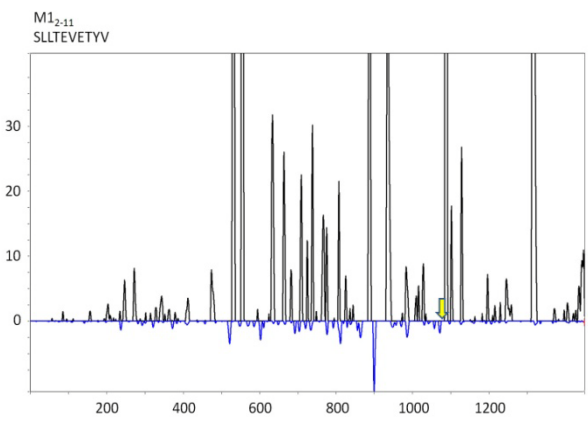
M1 2-11
SLLTEVETYV
30
20
10
0
200
400
600
800
1000
1200

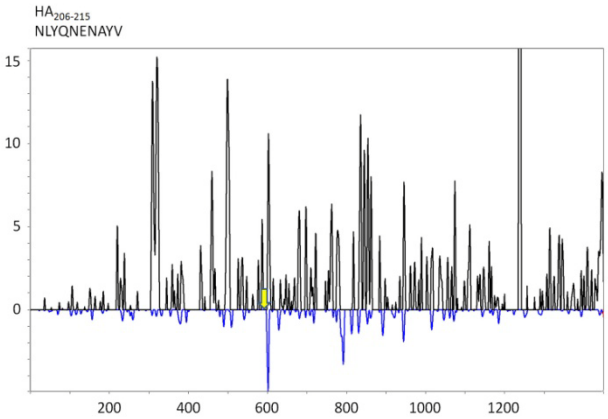
HA 206-215
NLYQNENAYV
15
10
5
0
200
400
600
800
1000
1200

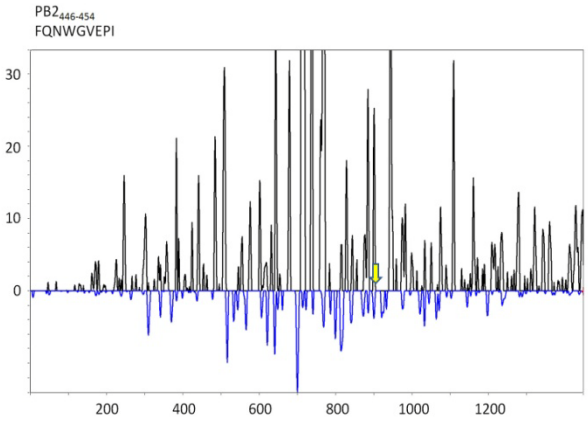
PB2 446-454
FQNWGVEPI
30
20
10
0
200
400
600
800
1000
1200

Figures S12. Negative detection in naïve (uninfected) BEAS cells of the eight IAV peptides synthesized that were detected in 18 hour PR8 infection (Fig. S10). The detection plots are of the same character as Fig. S2 with the predicted position (now using the naïve sample's elution polynomial) of the IAV peptide in the naive BEAS sample marked with an arrow.

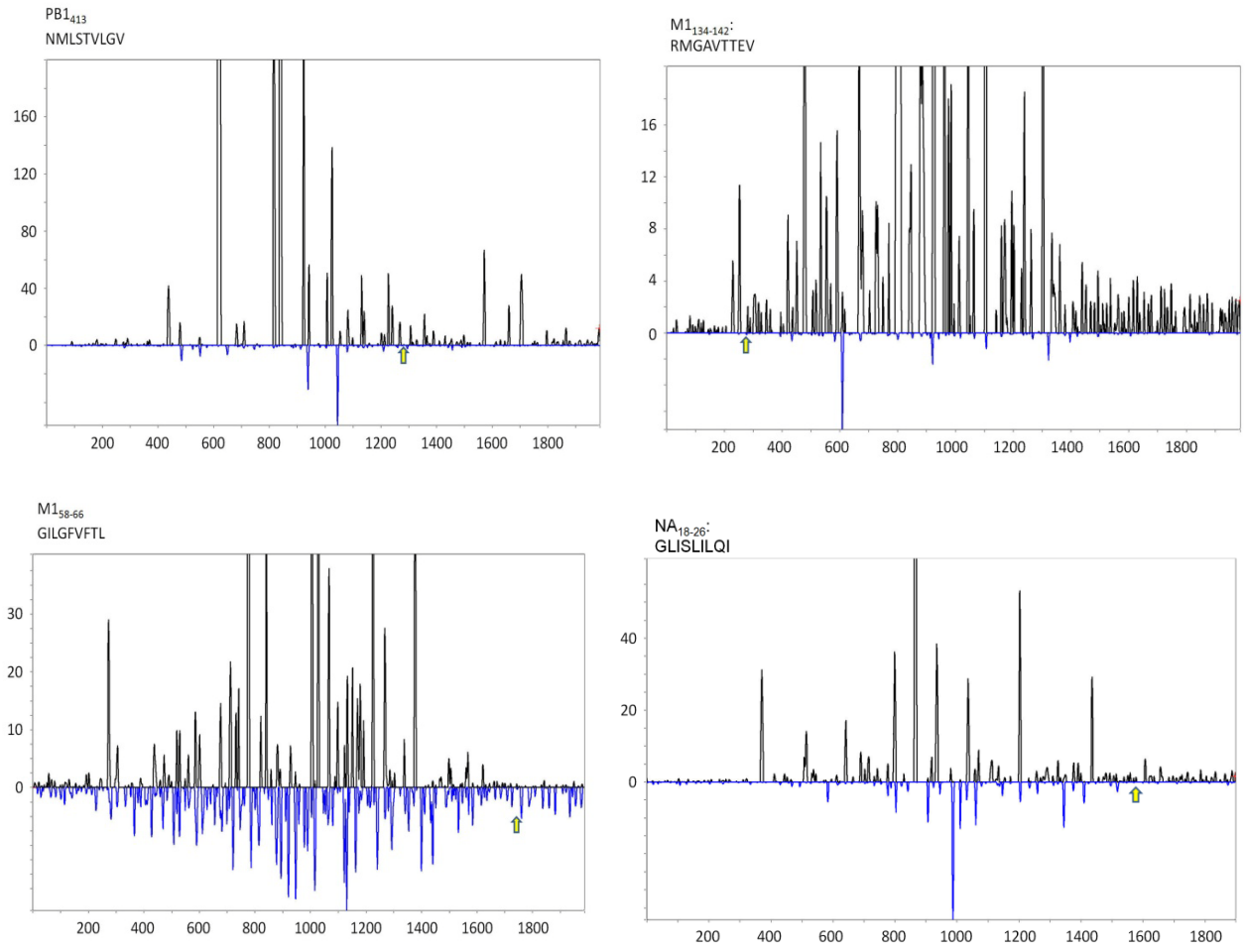

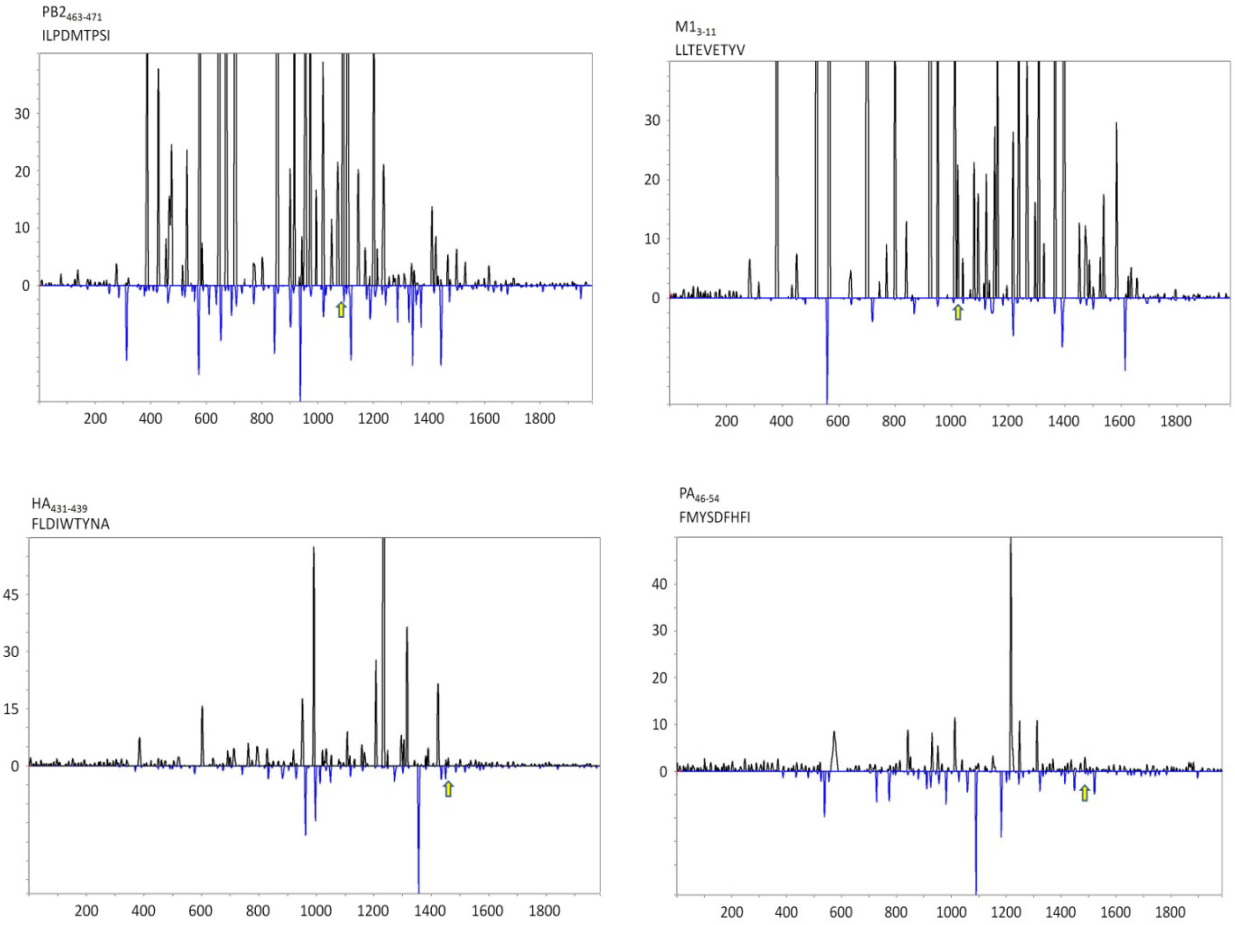
PB2463-471
ILPDMTPSI
30
20
10
0
200 400 600 800 1000 1200 1400 1600 1800
M13-11
LLTEVETYV
30
20
10
0
200 400 600 800 1000 1200 1400 1600 1800
HA431-439
FLDIWTYNA
45
30
15
0
200 400 600 800 1000 1200 1400 1600 1800
PA46-54
FMYSDFHFI
40
30
20
10
0
200 400 600 800 1000 1200 1400 1600 1800

Figures S13. Detection of IAV strain A/X-31 peptides from 1.67 million 18 hour infected BEAS cells. This strain shares core genes from PR8 but has different HA and NA genes. Same format for detection chromatogram as previously described (arrows marking predicted elution positions).

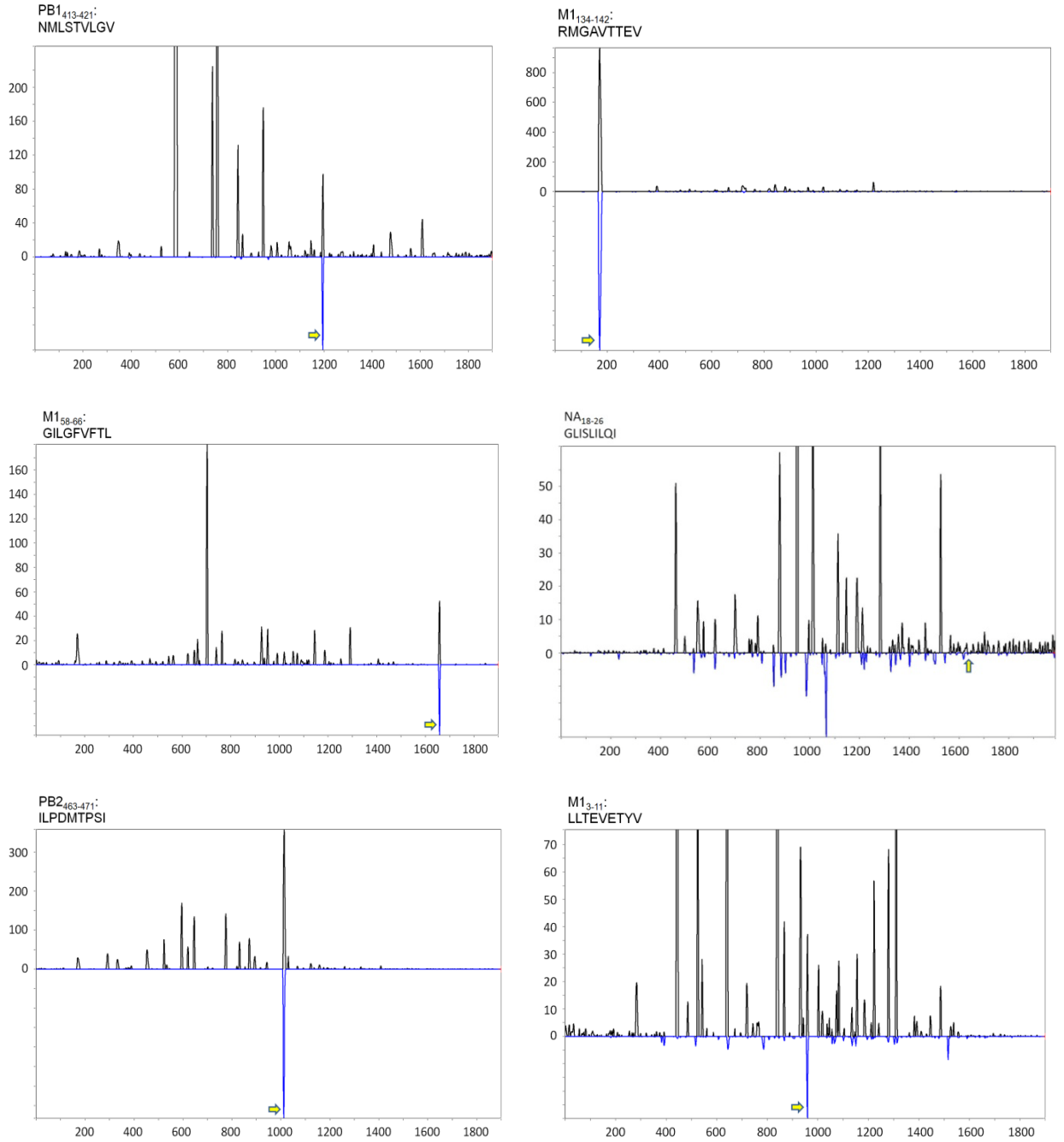

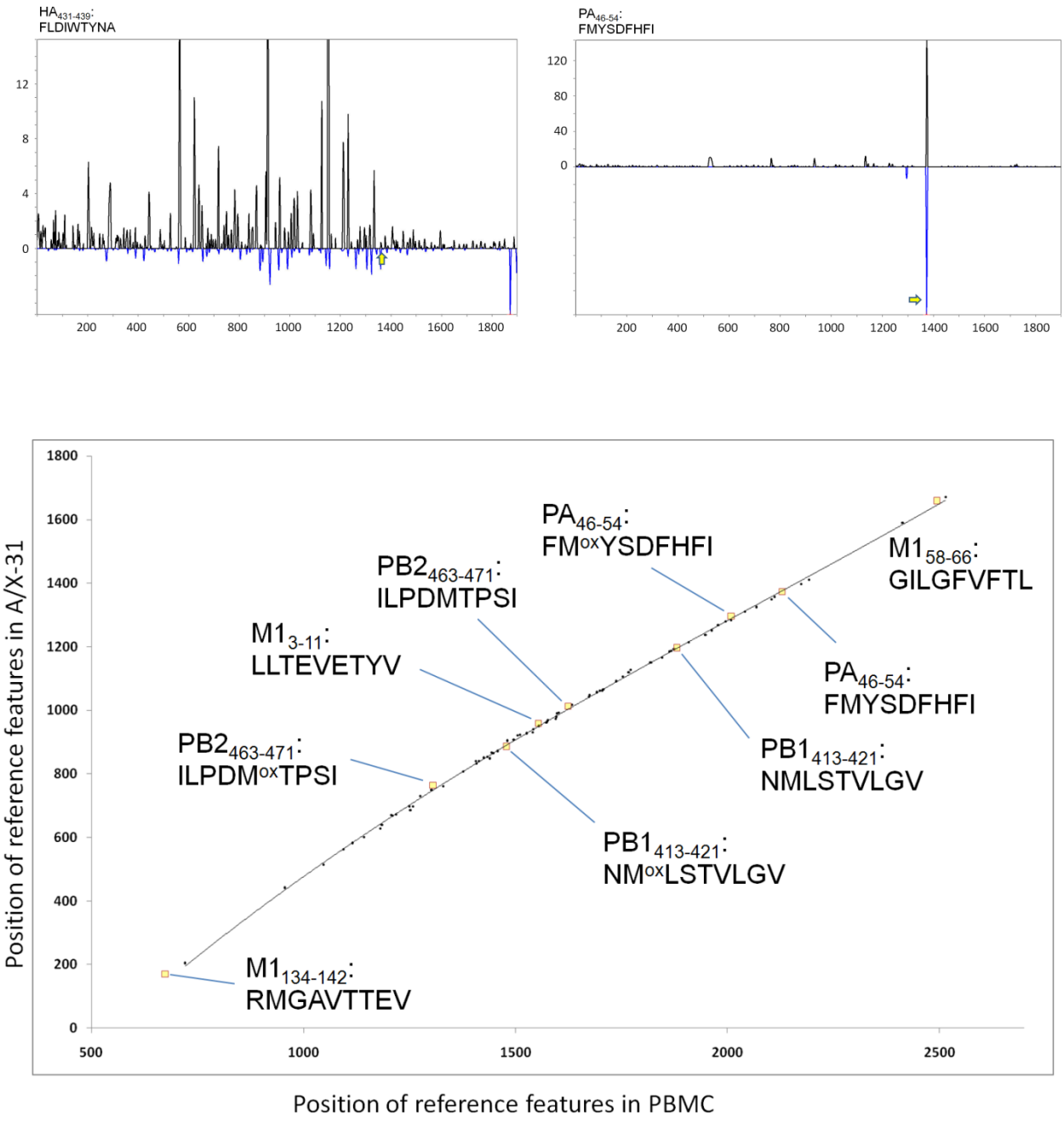

Figure S13a (above). Elution map for detected IAV peptides (including methionine oxidized variants).

Figures S14. Detection of IAV strain A/Victoria/3/75 peptides from 3.3 million 18 hour infected BEAS cells. Neither the detected HA and NA epitopes from PR8 nor the peptide ILPDMTPSI from the internal PB2 protein are present in this strain.

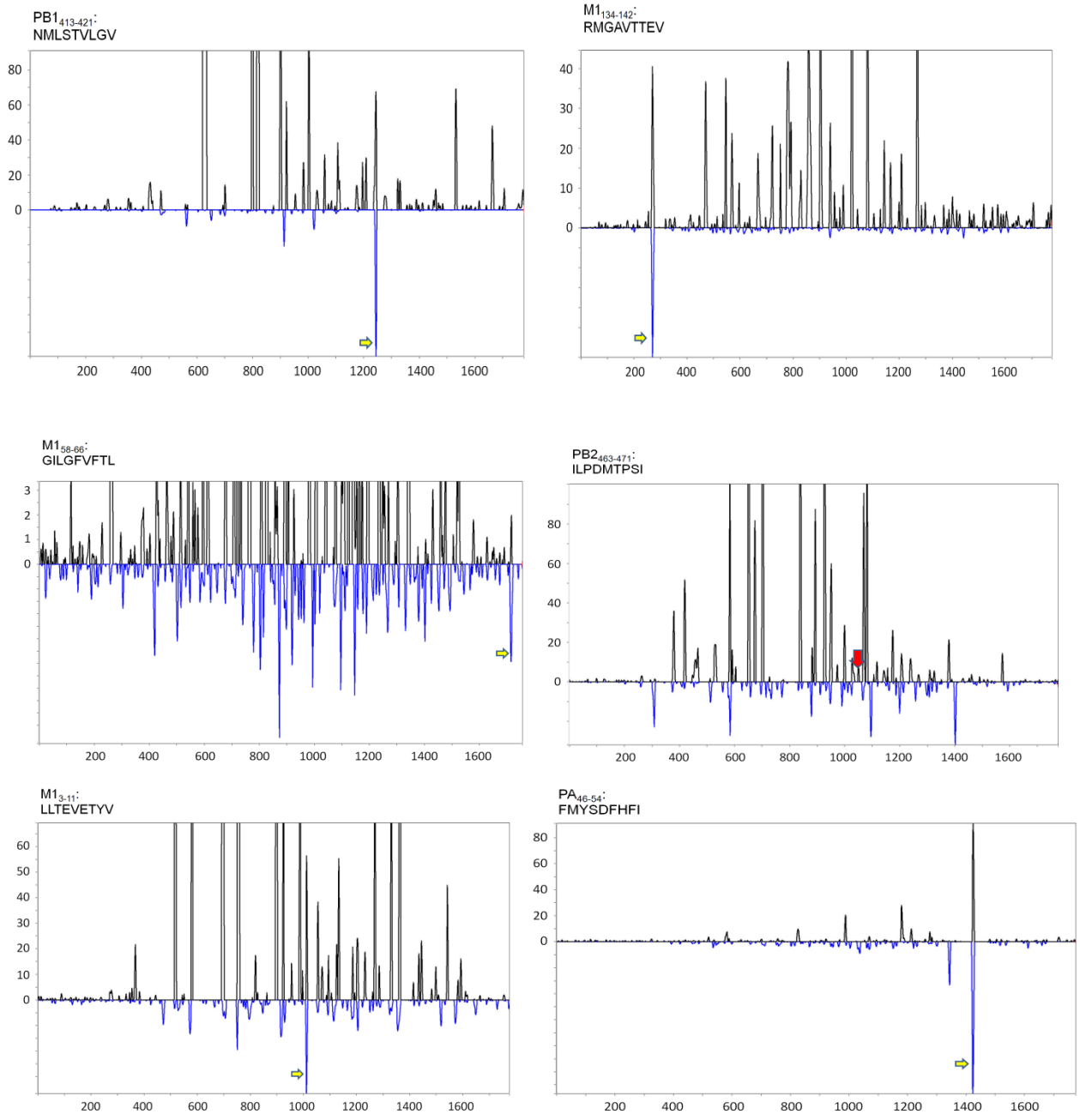

Figures S15a. **Normal Human Bronchial Epithelial cell (NHBE-Lonza) characterization and IAV infection. (A)** NHBE (Lonza) cells expressed CD326 (EpCam) lung epithelium marker. **(B)** HLA-A*02 expression analysis of BEAS-2B HLA-A02 cells (First panel) compared to NHBE (Lonza) cells (second and third panels) by flow cytometry. We selected HLA-A*02 positive NHBE (Lonza) cells for IAV infection (third panel). **(C)** HLA-A*02 positive NHBE cells were used for IAV infection. Time course of IAV infection was determined by intracellular M1 staining followed by flow cytometric analysis.

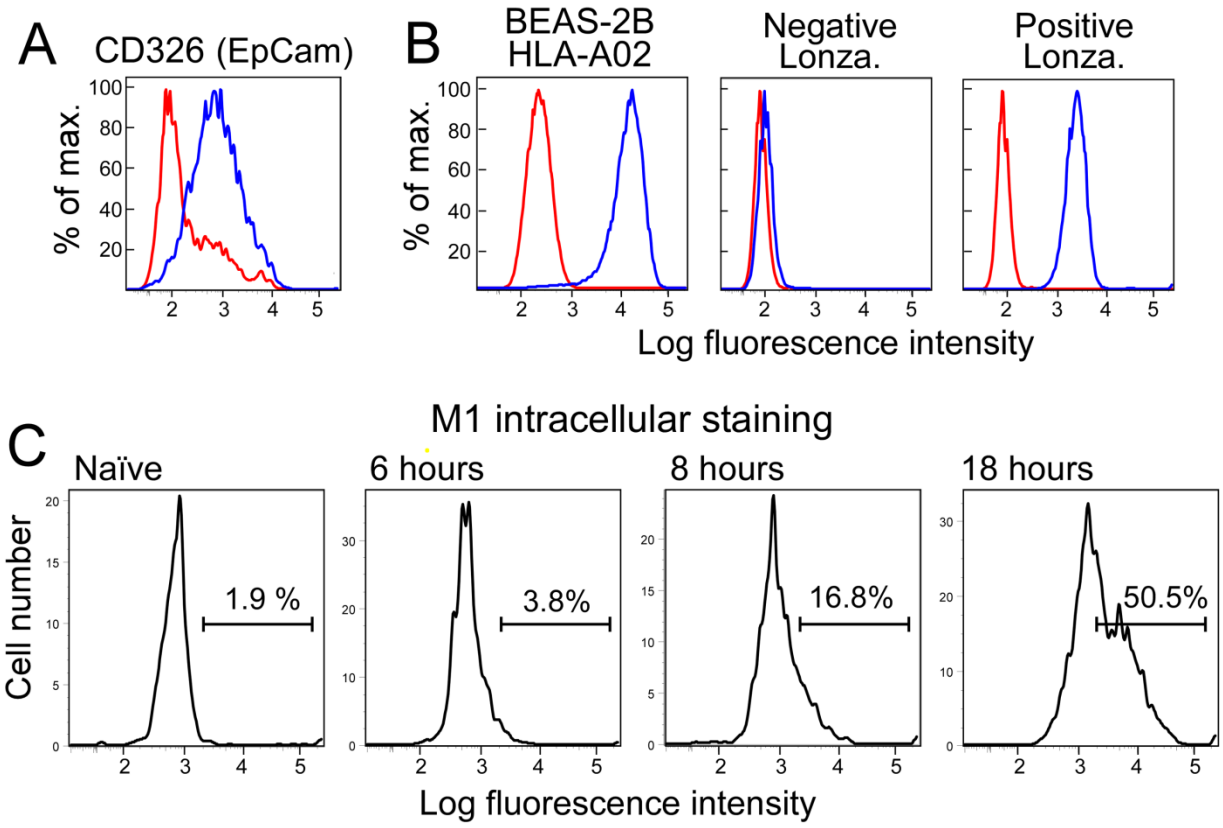

Figures S15b. MS^3 detection of peptides from PR8 infection of primary HLA-A02:01 lung tissue from Lonza. The M1$_{134-142}$ peptide RMGAVTTEV generates MS^3 spectra dominated by neutral losses and cannot be detected by MS^{3}with high sensitivity.

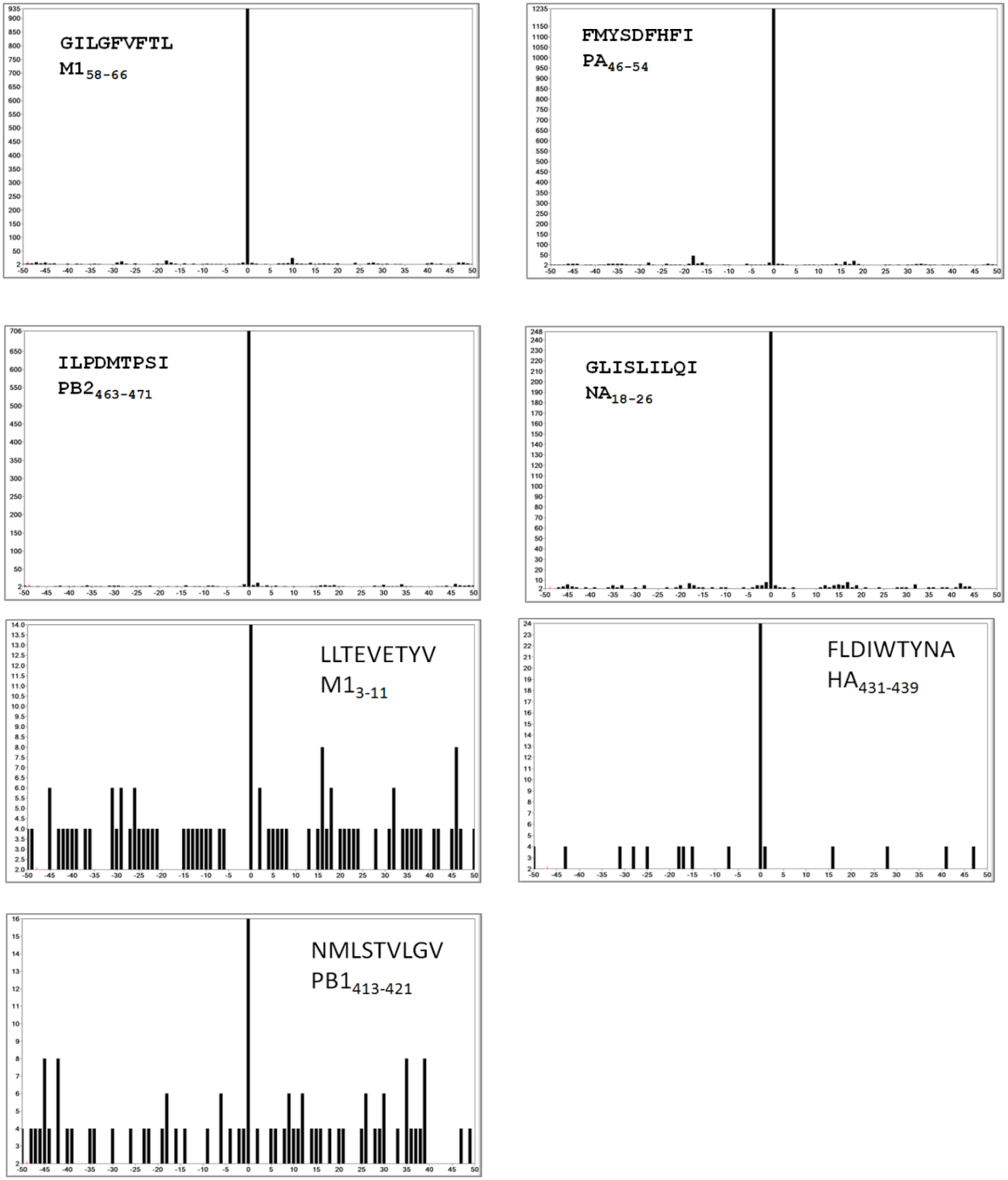

Figure S16. Poisson segmented LC-DIAMS detection does not identify the AIMDKNIIL peptide in naïve BEAS cells. Since this detection was made without the synthetic peptide there is no well defined elution map point to mark with an arrow. However, throughout the chromatogram the naïve BEAS sample produces no detection signature (coincident XIC and Poisson peaks) even at very low ion intensities (compare with Fig. 2A of the manuscript).

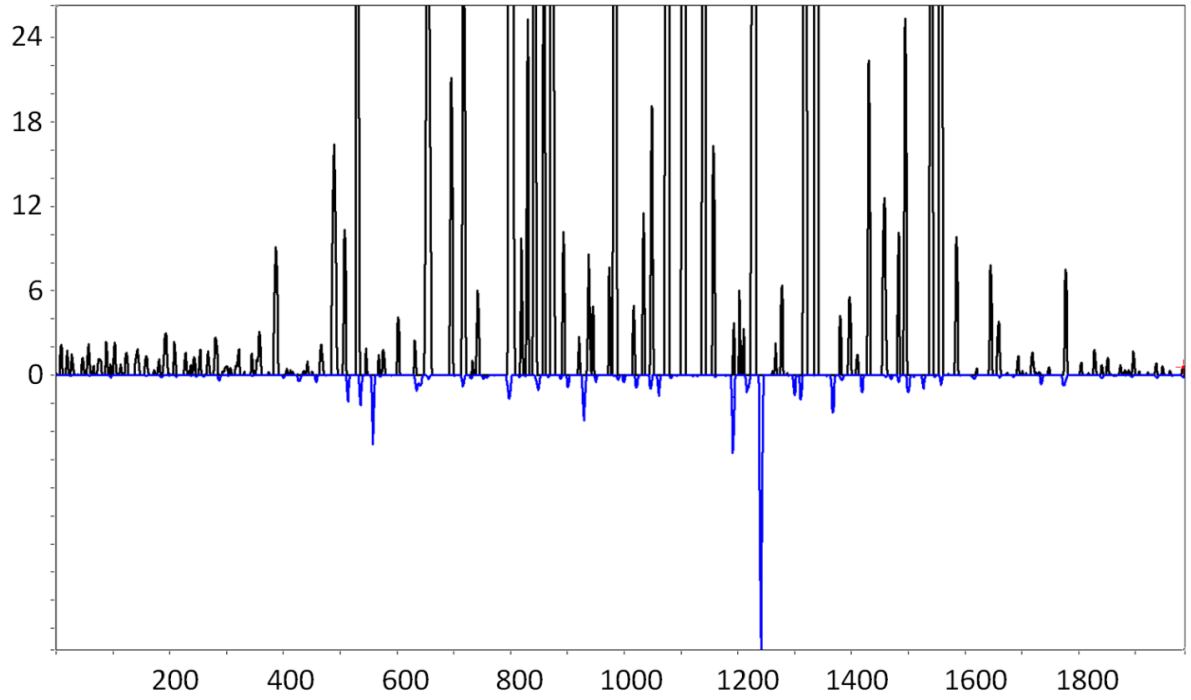

Figure S17. Poisson segmented LC-DIAMS detection of $M1_{59-66}$ peptide ILGFVFTL using in silico model of fragmentation and manual assignment of high energy band transmitting around m/z 455.28 (MS^2 spectrum) at the elution position of coincident XIC and Poisson peaks. **A**. Detection chromatogram using in silico model (3 b-ion fragments) with Kangas/Petritis elution position marked with arrow. **B**. High energy band at scan 1296 and fragment assignments.

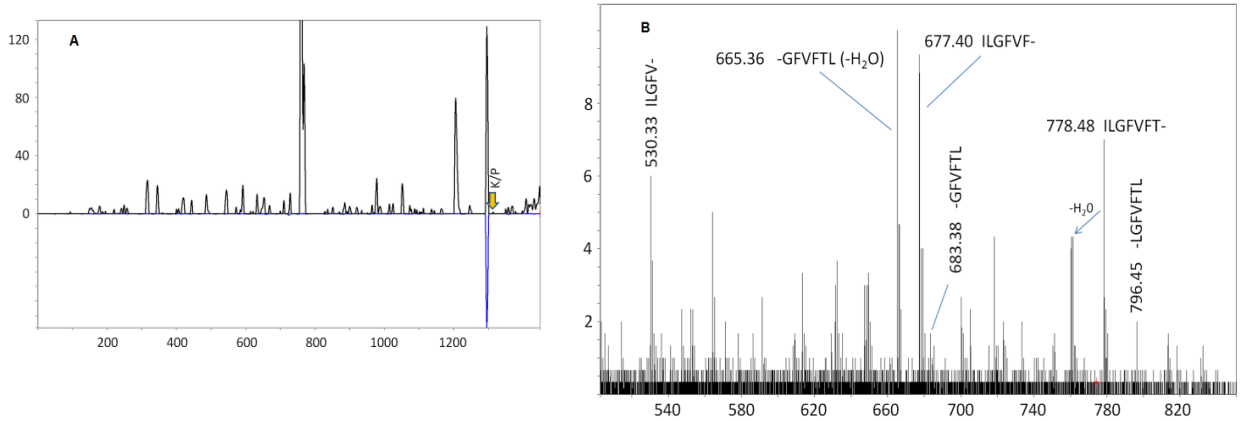

Figure S18a. Attenuation of viral infectivity by UV irradiation assayed by intracellular M1 stain. Red trace is naïve HLA-A*02:01^{+} BEAS cells, blue trace is intracellular M1 staining after 18 hour infection with 10 EID_{50} PR8. **A**. Normal infection (untreated virus). **B**. UV irradiated for 90 min. **C**. γ irradiated, 10000 roentgen dose.

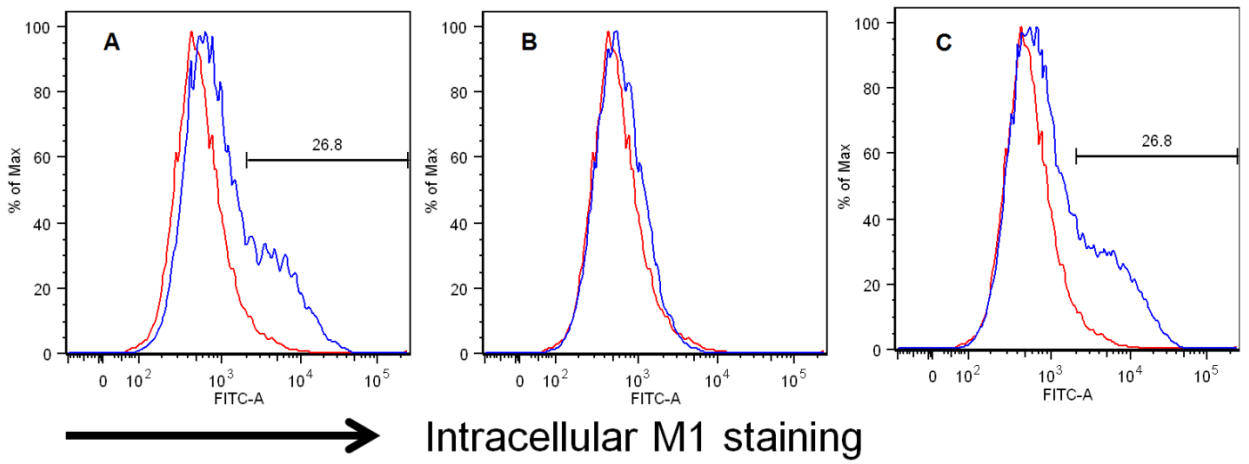

Figure S18b. Viral infectivity after UV irradiation is different for BEAS cells compared to monocyte-derived DCs. A. Poisson detection chromatogram for IAV $NS1_{122\text{-}130}$ peptide AIMDKNIIL after 18 hour infection of HLA-A*02:01^{+} BEAS cells with 10 EID_{50} UV irradiated PR8 virus shows no detection signature (expected elution by Kangas/Petritis NET utility marked with arrow). **B.** Infection of 1 million moDCs with 10 EID_{50} UV irradiated PR8 shows strong AIMDKNIIL signature.

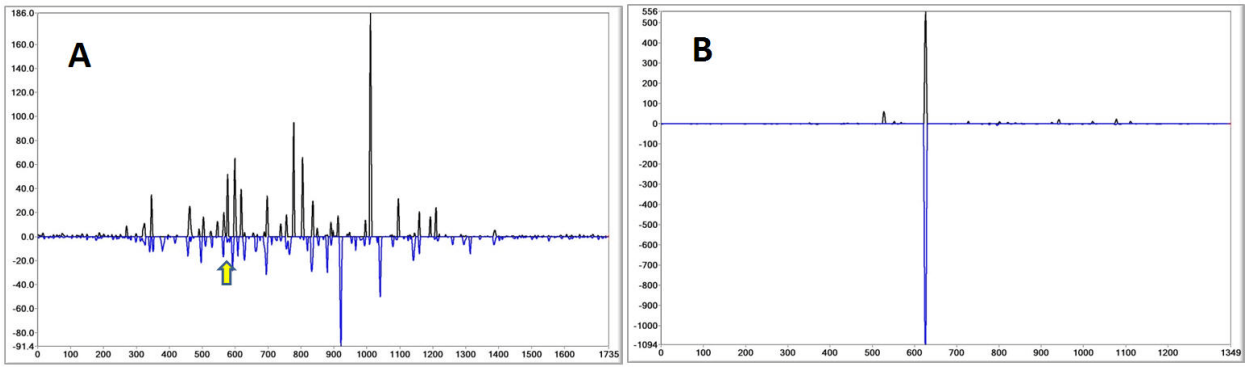

Figure S19a. UV irradiated virus still infects monocyte-derived DCs by surface HA. A. Naïve moDCs did not show surface HA by FACS analysis after staining with anti-HA mAb. **B**. HA surface staining by 10 EID_{50} PR8 virus after 18 hour infection (blue trace). Naïve trace (black) shown for comparison. **C**. HA surface staining by 10 EID_{50} 90 minute UV irradiated PR8 virus after 18 hour infection (blue trace). Naïve trace (black) shown for comparison.

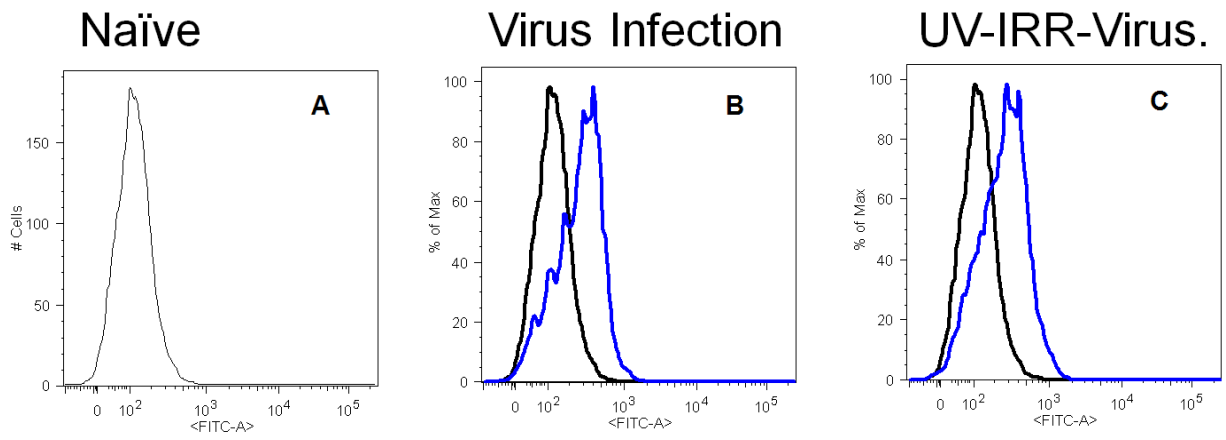

Figure S19b. Marker analysis of monocyte-derived DCs prior to infection. Monocytes were isolated by plastic adherence and were differentiated with GM-CSF and IL-4 (100ng/ml). Black: isotype control.

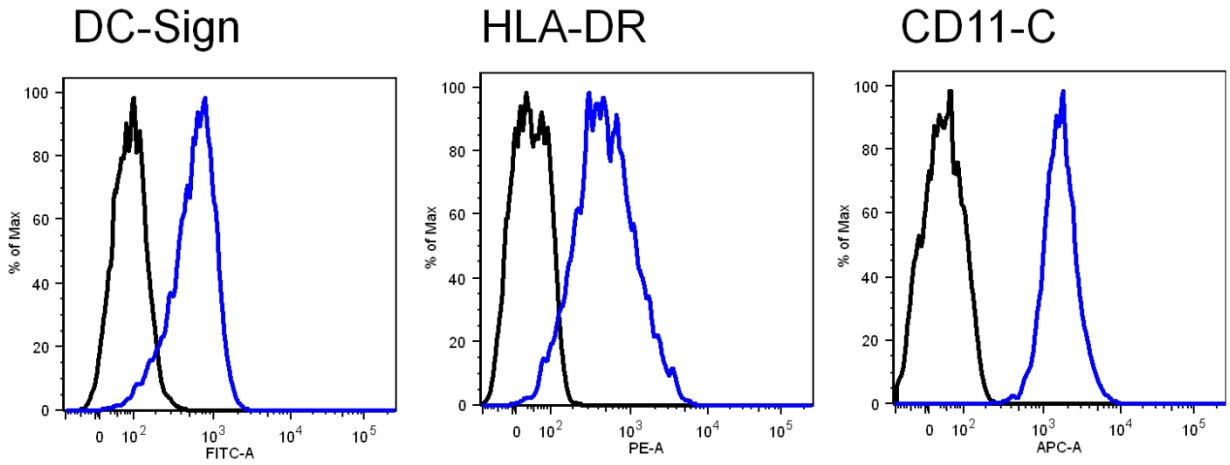

Figure S19c. Exposure of naïve moDCs to untreated or UV-irradiated virus induces phenotypic markers of DC maturity. For all three panels: red trace is naïve moDCs, blue trace is 18 hour infection with 10 EID_{50} PR8 virus, black trace is 18 hour infection with 10 EID_{50} of 90 min UV irradiated PR8 virus.

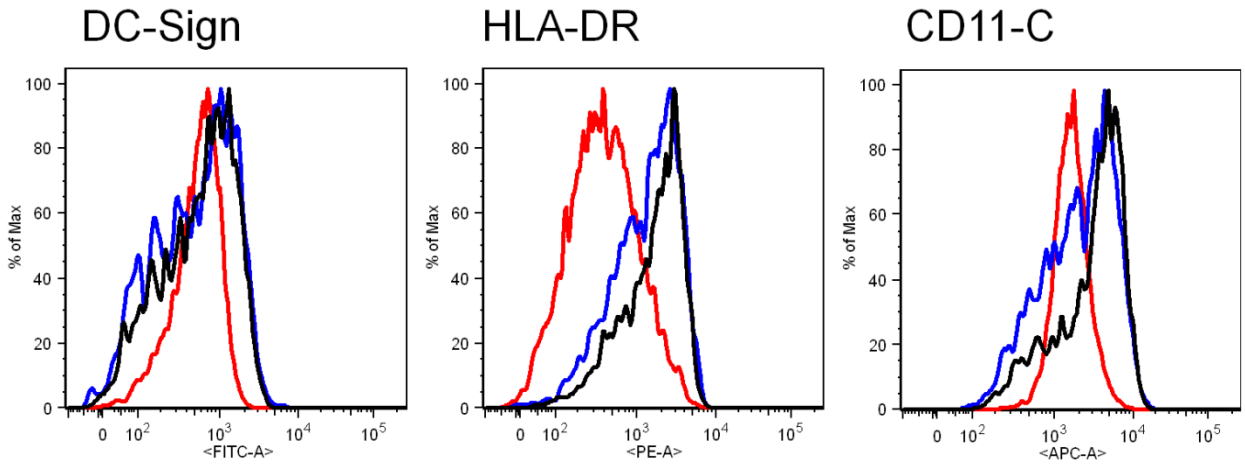

Figures S20a. HLA-A02 monocyte-derived DCs generate only unlabeled IAV peptides after 18 hour culture with SILAC labeled, IAV X-31 infected at 10 EID_{50} and apoptotic LAZ 468 cells. Poisson detection chromatograms for unlabeled IAV X-31 peptides:

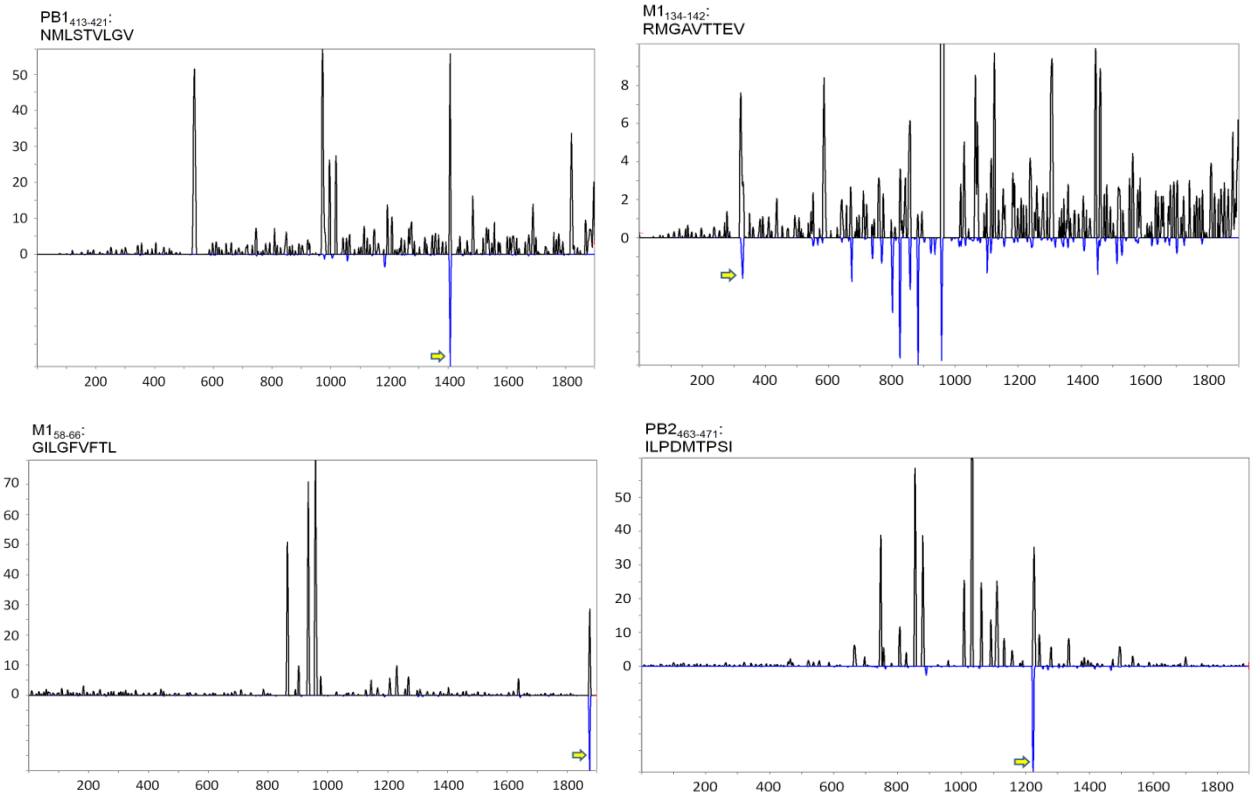

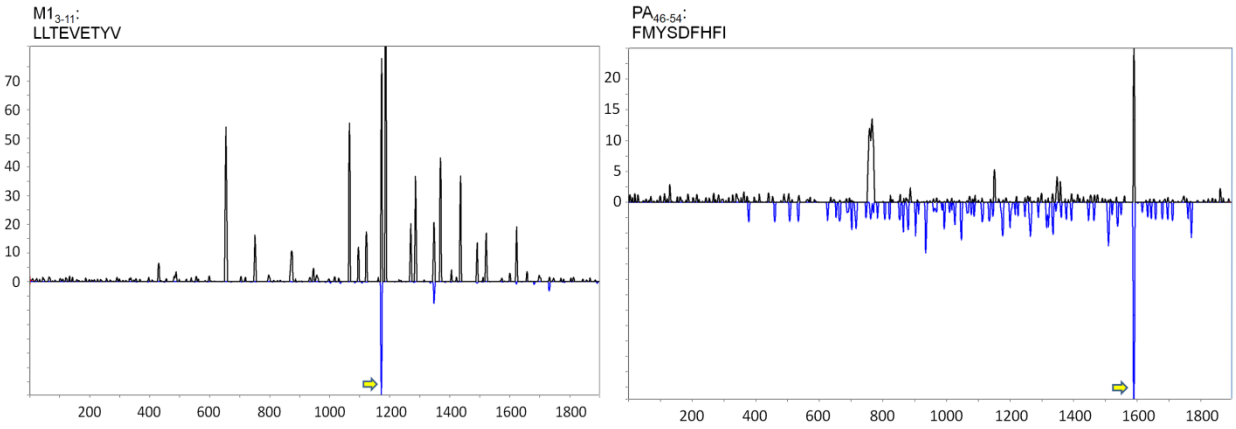

Figure S20b. **Elution map of unlabeled IAV peptides detected in moDCs fed SILAC labeled, IAV X-31 infected, apoptotic A2$^-$ LAZ cells plotted over the elution line of endogenous peptides.**

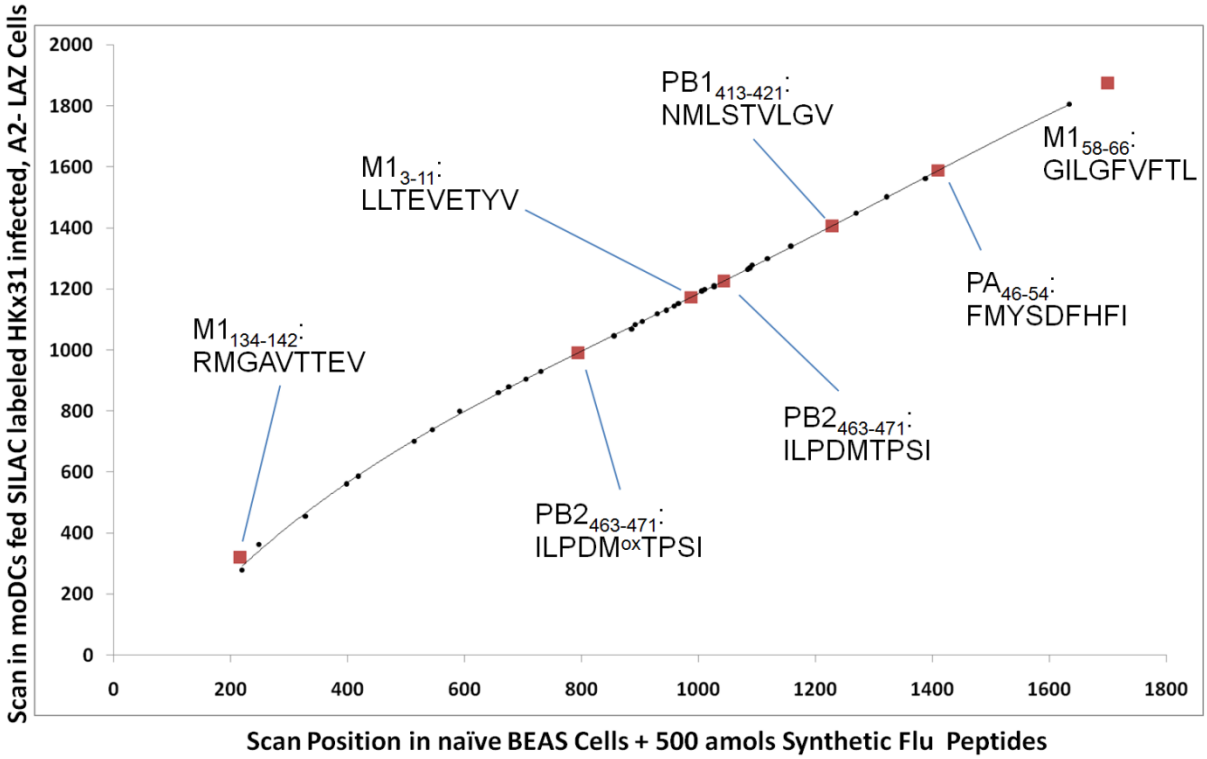

Figures S20c. No evidence for co-eluting isotope-labeled IAV peptides in moDCs fed SILAC-labeled IAV infected A2$^-$ LAZ cells. The mass spectra at the elution positions of unlabeled IAV peptides do not show evidence for co-eluting isotope labeled forms (x axis: m/z; y axis: ion events). Figure 4B of manuscript shows the same for $NS1_{122-130}$ peptide AIMDKNIIL**.**

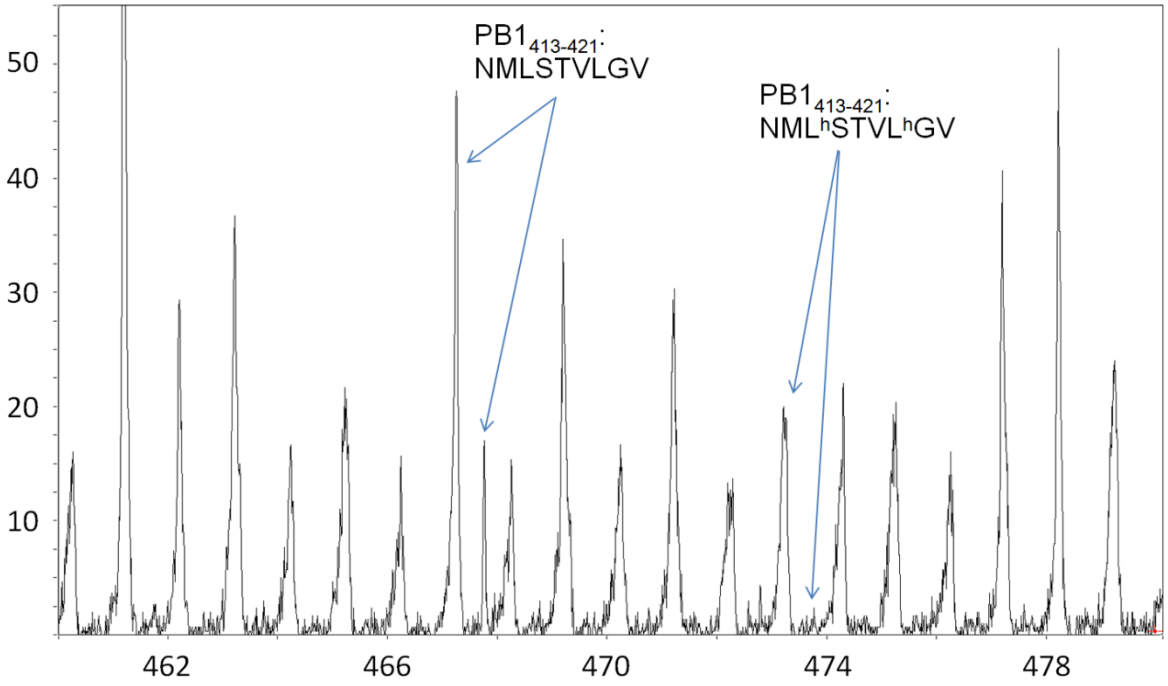

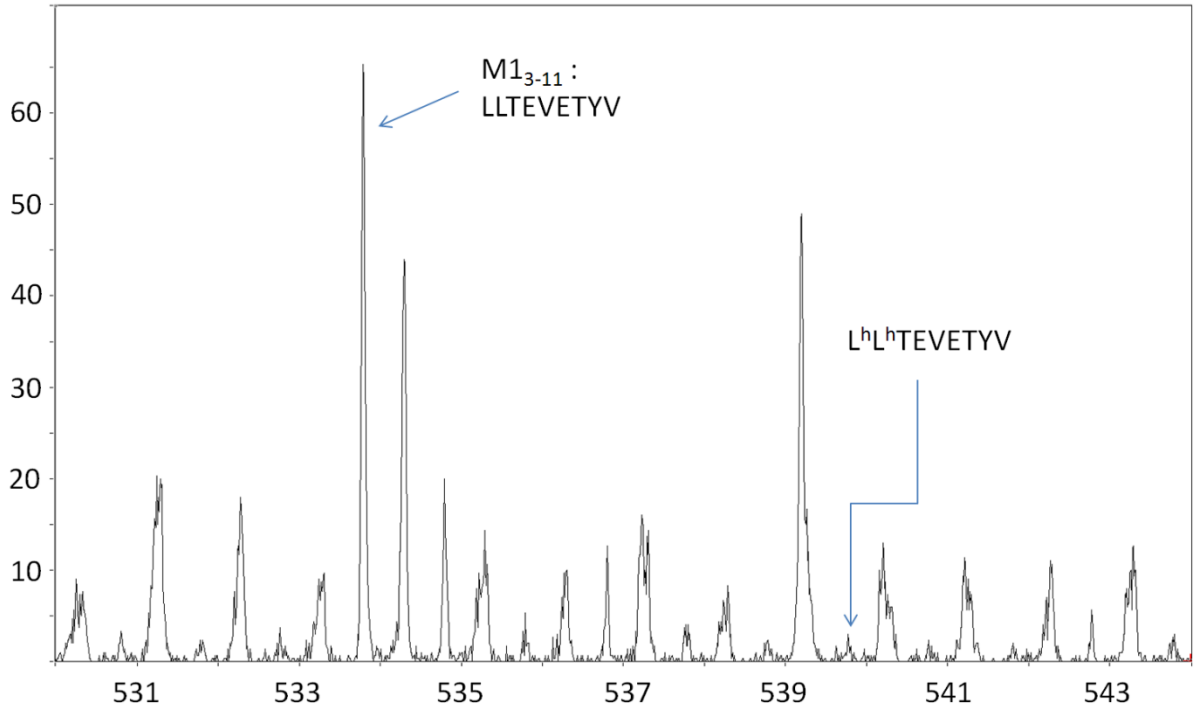
M1$_{3-11}$:
LLTEVETYV
L^{h}L^{h}TEVETYV
60
50
40
30
20
10
531
533
535
537
539
541
543

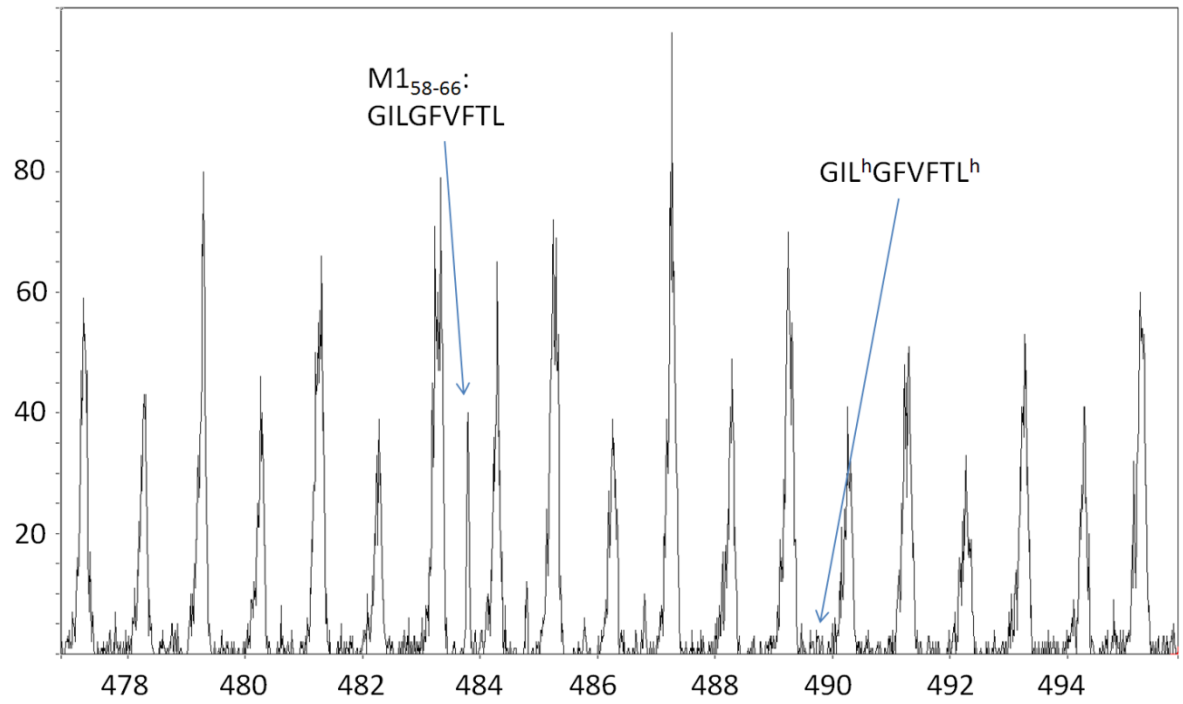
M1$_{58-66}$:
GILGFVFTL
GIL^{h}GFVFTL^{h}
80
60
40
20
478
480
482
484
486
488
490
492
494

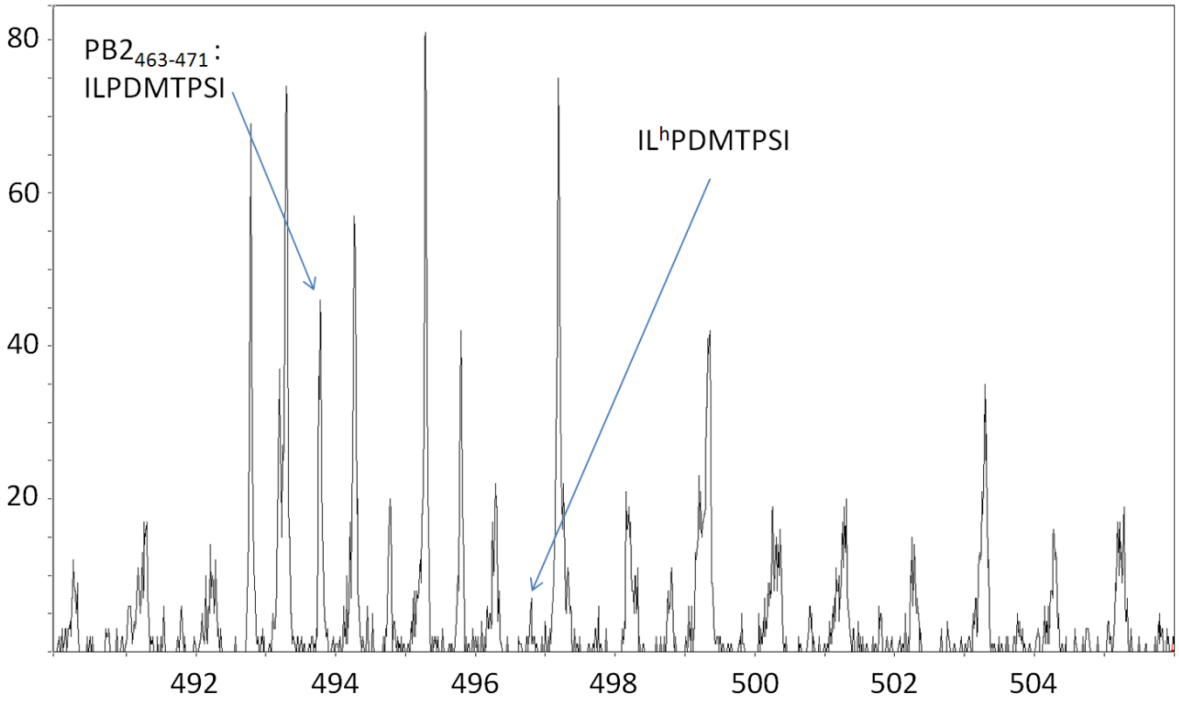

Above. The spectral region around m/z 495 at the elution of ILPDMTPSI is crowded and the identification of a isotope labeled analog is obscured by isotope peaks of endogenous peptides.

Figures S21. MS^3 quantification of $M1_{58-66}$ in peptide loaded uninfected BEAS cells using isotope labeled analog. The MS^3 Poisson signature ratio for an equimolar solution of light and heavy forms of $M1_{58-66}$ gave 0.8 for light/heavy (See Quantitation, MS^3 quantitation of $M1_{58-66}$ above). **A, B.** 3.3 million naïve BEAS cells were incubated with 1 ng/ml of light of $M1_{58-66}$ (m/z 483.79) for 1 hour and cells were washed, lysed and A2 pMHCI complexes affinity isolated. 500 amols of heavy $M1_{58-66}$ (m/z 486.80) was added at the acid elution step and eluted peptides analyzed by nanospray MS^3. MS^3 Poisson detection signatures for light (**A**) and heavy (**B**) forms give a ratio of 10/310 (subtracting backgrounds) and using the 0.8 normalization we have 10/(310 x 0.8) x 500 amols = 20 amols of light $M1_{58-66}$. Translated into copies per cell, there are 3.6 copies/cell from 1 ng/ml loading. **C, D.** Same as before except loading was 10 ng/ml for 1 hour. This gives 28 copies/cell.

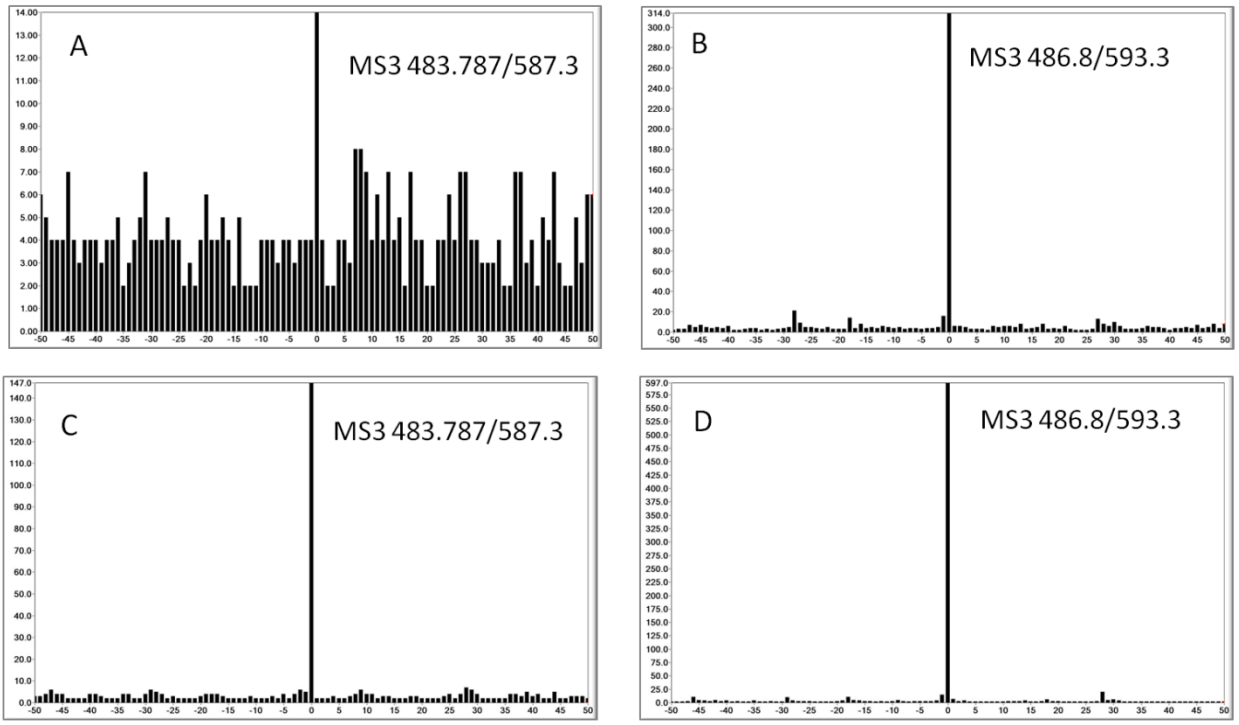

Figure S22. HLA-A02 positive donor memory immune responses to conserved, HLA-A02 restricted IAV epitopes. (**A**) Immune recognition of the conserved HLA-A*02:01 restricted IAV peptides was tested in an IFNγ Elispot assay. PBMC isolated from HLA-A*02:01-positive healthy donors were stimulated with 10 µg/ml respective peptide for 18 hours. In panel A, spots are graphed and presented as SFUs per million PBMC. SFUs of single donors are represented as dots, with a horizontal line corresponding to the mean of ten donor samples. Robust responses are defined as > or = to 50 spots above background (0 normalized). All epitope analyses were with 10 donors, except for $PB1_{501-509}$ where 7 individuals were examined.(**B**) Elispot well images from a representative donor (2×10^5 cells/well) is shown in panel B.

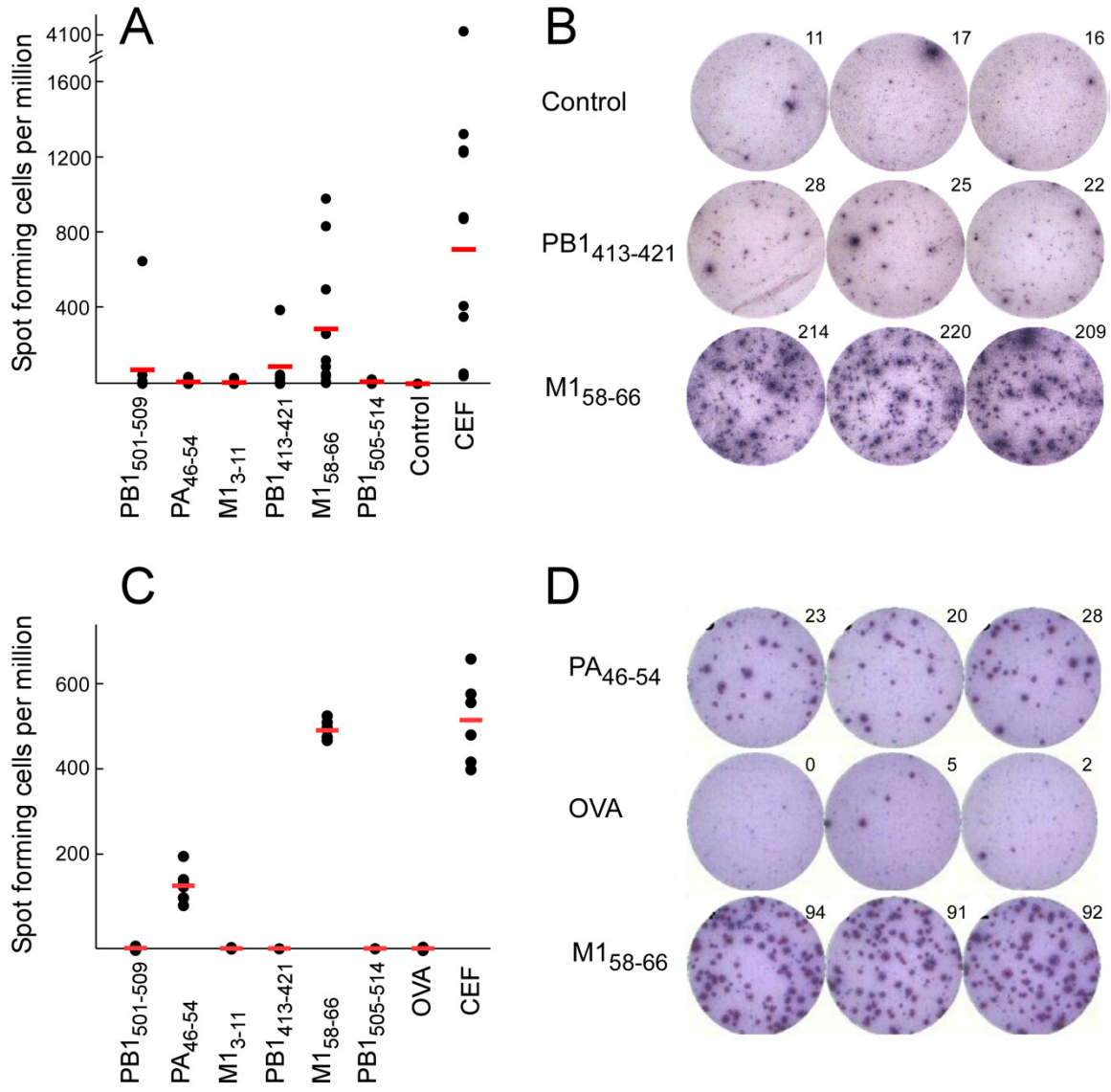

(**C**) Naive HLA-A02 restricted IAV responses were determined in HLA-A2.1 transgenic mice post non-lethal IAV infection. Splenocytes were isolated 4 weeks post non-lethal IAV infection and were stimulated with 10µg/ml respective peptide for 18 hours. SFU of wells were represented as dots, with a

horizontal line corresponding to the mean of responses. (**D**) Elispot well images from a representative mouse are shown in panel D.

Figures S23. Conservation analysis of the detected IAV peptides. For each peptide, the first panel is the block entropy analysis of the detected IAV peptide. Sequence positions depict the global sequence alignment among the selected IAV sequences and may be different from the Influenza/PR8/34 sequence positions described in Table 1 of the manuscript. The second panel provides the predicted binding affinities (IC_{50} in nM) using netMHCpan 2.8 to eight HLA class I alleles while the third panel lists the IAV peptides required to cover 99% of the IAV sequences. Full length IAV sequences were selected for this analysis among the IAV viruses that infected humans from the years 1902 - 2014.

Peptide	HLA binding prediction							
	A*0101	A*0201	A*0301	A*1101	A*2402	B*0702	B*0801	B*1501
FMYSDFHFI	9843.76	2.41	10708.04	8155.94	457.31	23189.50	1616.02	502.34

#	Peptide	Frequency	Accumulated frequency	Number of sequences
1	FMYSDFHFI	99.75%	99.75%	10782

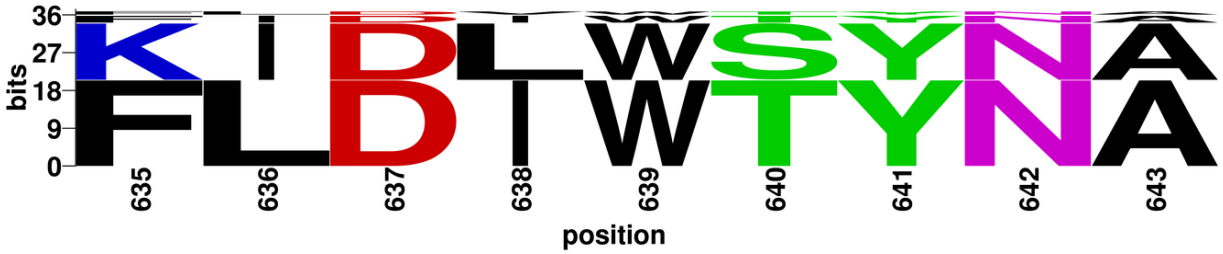

Peptide	HLA binding prediction							
	A*0101	A*0201	A*0301	A*1101	A*2402	B*0702	B*0801	B*1501
FLDIWTYNA	1433.7	5.22	22639.13	25981.74	25255.56	31814.04	11598.39	25296.31

	3							
KIDLWSYNA	8363.63	192.91	12851.06	9617.52	33001.89	37240.24	28616.16	28546.87
FIDIWTYNA	1302.06	19.65	23252.31	20532.96	29575.92	30672.6	16263.43	27881.11
FLDVWTYNA	1329.11	4.49	23041.44	25723.85	26046.48	31071.08	10209.54	23679.86
FIDVWTYNA	1317.61	17.87	23891.93	20519.64	30352.03	30485.33	15336.62	27242.09

#	Peptide	Frequency	Accumulated frequency	Number of sequences
1	FLDIWTYNA	54.94%	54.94%	10817
2	KIDLWSYNA	36.44%	91.38%	7174
3	FIDIWTYNA	4.95%	96.33%	975
4	FLDVWTYNA	2.51%	98.85%	495
5	FIDVWTYNA	0.48%	99.33%	95

Peptide	HLA binding prediction							
	A*0101	A*0201	A*0301	A*1101	A*2402	B*0702	B*0801	B*1501
LLTEVETYV	19687.96	6.72	24177.19	28110.71	34048.31	31369.00	23861.71	14065.25

#	Peptide	Frequency	Accumulated frequency	Number of sequences
1	LLTEVETYV	99.56%	99.56%	14556

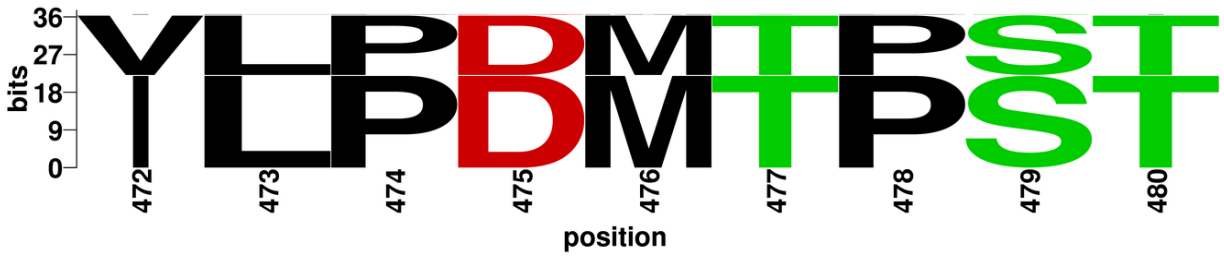

Peptide	HLA binding prediction							
	A*0101	A*0201	A*0301	A*1101	A*2402	B*0702	B*0801	B*1501
ILPDMTPST	31918.87	125.44	32317.09	36589.99	29909.64	26949.21	28460.53	16379.1
VLPDMTPST	30988.81	208.55	32065.97	35337.93	31754.55	30568.88	29735.08	19440.72
ILPDMTPSI	23638.15	8.65	24396.88	29407.77	2385.49	16059.54	13203.57	4261.42
ILSDMTPST	27218.52	45.64	22475.85	29989.04	37615.62	19786.41	22764.15	6298.06
ILPDMTPSM	20325.62	37.34	21922.24	28174.67	8689.72	6561.55	9371.4	829.47
ILPDLTPST	31010.28	103.61	32553.99	36449.72	31971.73	28636.91	30324.78	17968.95

#	Peptide	Frequency	Accumulated frequency	Number of sequences
1	ILPDMTPST	58.77%	58.77%	6387
2	VLPDMTPST	38.31%	97.07%	4163
3	ILPDMTPSI	0.75%	97.83%	82
4	ILSDMTPST	0.51%	98.33%	55
5	ILPDMTPSM	0.39%	98.72%	42
6	ILPDLTPST	0.17%	99.09%	18

Peptide	HLA binding prediction							
	A*0101	A*0201	A*0301	A*1101	A*2402	B*0702	B*0801	B*1501
NMLSTVLGV	21657.02	9.40	16025.53	19534.34	16349.00	24684.71	4014.10	6563.68

#	Peptide	Frequency	Accumulated frequency	Number of sequences
1	NMLSTVLGV	99.66%	99.66%	10630

Peptide	HLA binding prediction							
	A*0101	A*0201	A*0301	A*1101	A*2402	B*0702	B*0801	B*1501
GILGFVFTL	31899.17	15.03	16388.49	13550.48	10417.20	25456.10	13223.29	10746.92

#	Peptide	Frequency	Accumulated frequency	Number of sequences
1	GILGFVFTL	99.66%	99.66%	10630

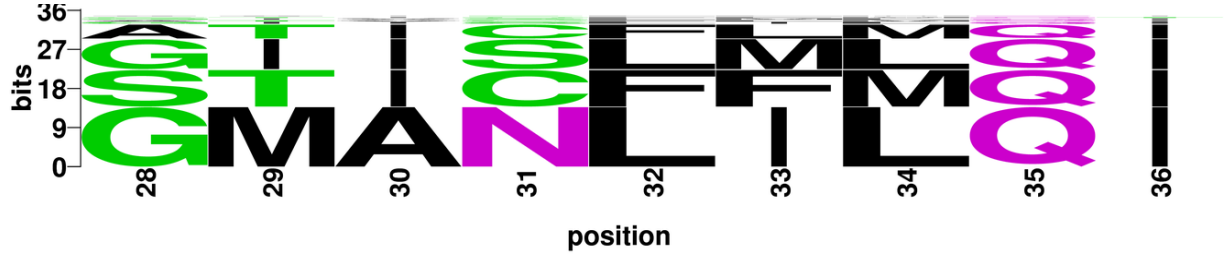

Peptide	HLA binding prediction							
	A*0101	A*0201	A*0301	A*1101	A*2402	B*0702	B*0801	B*1501
GMANLILQI	23382.25	27.95	11394.39	14093.27	4573.05	20521.41	13527.19	681.75
STICFFMQI	12490.26	154.05	5983.58	715.62	1886.99	23598.79	3864.51	3116.69
GIISLMLQI	30617.22	341.5	15867.48	13316.76	13093.17	26549.53	22588.96	4347.87
ATICFLMQI	16702.12	137.3	9089.58	2256.3	5730.95	27190.55	14574.94	5599.18
GIISLILQI	32029.91	184.42	18260.78	15987.59	11950.75	28917.76	19077.73	4433.04
ATVCFLMQI	19265.88	420.44	12219.17	3546.5	10874.88	29820.46	18130.26	9458.91
GIVSLMLQI	32496.62	883.62	19131.27	16762.59	18767.76	28343.45	26643.33	6747.07
STICFFMQT	20990.52	2470.57	10328.2	1317.17	31549.75	32735.88	15768.73	12380.34

AAICFLMQI	29294.07	643.25	16968.79	8233.62	10735.3	23272.2	9137.31	7653.72
GLISLILQI	31871.58	20.27	16629.46	20775.87	9116.57	30034.81	14018	2441.98
ATICFLTQI	18949.57	188.74	13770.11	4895.54	7695.07	24489.18	16736.68	4499.24
STICFFMQV	8031.16	27.27	4578	525.03	10447.9	25175.89	4382.25	5336.14
STICFLMQI	12612.76	119.4	8936.96	1721.15	3581.63	25163.36	9684.14	5288.16
TTICFLMQI	16144.74	339.43	12603.07	2995.71	5340.71	30772.65	13426.29	9799.98
GIVSLMLQV	28489.49	185.34	16988.82	14313.49	30226.17	30945.93	28316.16	10035.73
GAIAVLIGI	33613.1	1345.14	24456.08	17784.24	22276.6	31694.83	28346.81	10462.84
STICFFIQI	16921.13	306.27	9483.09	1449.41	5808.8	29615.32	7976.69	6231.43
GMVSLMLQI	31783.07	74.76	15385.49	16643.32	7290.47	25350.56	18566.39	1186.04
GIISLLLQI	30689.18	139.33	17250.91	15558.41	9529.99	28616.16	19678.8	4450.29
GMANLMLQI	21491.52	48.41	9716.78	11929.95	5628.03	18339.99	17417.08	742.39
GTISLILQI	19962.09	963.02	16261.32	8628.26	5480.08	26080.6	22653.83	4954.74
GIANLILQI	24071.74	321.46	15620.99	14431.21	15785.45	22777.21	21542.27	4930.89
GLANLILQI	23735.79	30.26	13986.18	19393.88	10724.27	24071.23	16370.07	2569.98
GMISLMLQI	29930.69	31.01	11988.69	12836.89	3803.33	23726.79	14720.59	612.39
STVCFFMQI	14904.09	388.74	8813.19	1259.92	4483.59	26434.31	5740.7	5402.02
STIGFFMQT	19212.58	2200.39	9380.94	1180.92	26701.63	29624.93	21009.85	9604.63
GTVSLMLQI	19432.51	3097.06	16664.4	8623.78	11428.72	26148.13	29851.77	7088
STICLFMQI	14364.69	337.52	10160.5	1904.32	1944.04	21574.23	5444.09	2763.2
GIINLILQI	30999.89	270.39	17565.65	15978.26	15317.21	28329.03	19731.89	4278.38
GTISLMLQI	17146.15	1395.77	13575.28	6119.84	6016.37	23627.14	25901.75	4268.07
GMTNLILQI	28587.99	98.78	17026.73	19414.02	8168.66	26176.43	16236.18	3047
GMANLILQV	18788.08	8.87	8886.44	12317.27	14973.92	22754.3	13424.97	1031.11
GIISLMLQV	26542.63	73.85	13689.6	11127.45	25573.98	29357.22	24402.17	7237.26
ATICFLMQV	11515.23	25.82	7621.41	1404.04	18574.03	28717.58	15789.9	8208.98
ATICLLMQI	18599.37	289.75	13395.67	5181.45	5746.41	25061.48	17544.76	5238.72
ATMCFLMQI	10201.92	25.01	3997.42	627.02	2233.37	18524.85	5863.23	3762.69
ATICFLIQI	20875.47	295.46	12232.93	3728.72	12344.76	32654.88	21257.94	9999.09
ETVCFLMQI	21707.22	5565.35	27761.62	13974.84	20263.7	35273.38	16066.15	20627.37
GMANLVLQI	22661.19	32.23	10789.09	13046.37	4828	19587.46	13546.38	560.73
STTCFFMQI	11184.79	1322.3	9871.28	1527.35	4866.65	26513.64	7883.51	11132.03
GVISLMLQI	29641.61	725.38	15841.75	9992.5	9923.76	20918.21	23463.59	4798
ATICFFMQI	16523.99	206.35	6331.61	964.96	3564.42	25679.34	7355.28	3413.3
GIASLMLQI	23103.59	422.26	13844.8	11739.16	13302.65	20750.27	23422	4952.81

#	Peptide	Frequency	Accumulated frequency	Number of sequences
1	GMANLILQI	38.17%	38.17%	7840
2	STICFFMQI	23.62%	61.79%	4852
3	GIISLMLQI	19.51%	81.31%	4008
4	ATICFLMQI	9.31%	90.62%	1912
5	GIISLILQI	1.54%	92.16%	317
6	ATVCFLMQI	1.17%	93.33%	240

7	GIVSLMLQI	1.06%	94.39%	218
8	STICFFMQT	0.93%	95.32%	190
9	AAICFLMQI	0.69%	96.01%	142
10	GLISLILQI	0.34%	96.34%	69
11	ATICFLTQI	0.27%	96.61%	55
12	STICFFMQV	0.23%	96.84%	47
13	STICFLMQI	0.22%	97.06%	45
14	TTICFLMQI	0.16%	97.22%	32
15	GIVSLMLQV	0.14%	97.35%	28
16	GAIAVLIGI	0.13%	97.48%	26
17	STICFFIQI	0.10%	97.58%	21
18	GMVSLMLQI	0.10%	97.68%	20
19	GIISLLLQI	0.09%	97.77%	18
20	GMANLMLQI	0.08%	97.84%	16
21	GTISLILQI	0.08%	97.92%	16
22	GIANLILQI	0.08%	98.00%	16
23	GLANLILQI	0.07%	98.07%	15
24	GMISLMLQI	0.07%	98.14%	14
25	STVCFFMQI	0.07%	98.21%	14
26	STIGFFMQT	0.06%	98.27%	13

27	GTVSLMLQI	0.06%	98.33%	12
28	STICLFMQI	0.06%	98.39%	12
29	GIINLILQI	0.05%	98.44%	11
30	GTISLMLQI	0.05%	98.50%	11
31	GMTNLILQI	0.05%	98.55%	11
32	GMANLILQV	0.05%	98.60%	10
33	GIISLMLQV	0.05%	98.65%	10
34	ATICFLMQV	0.04%	98.69%	9
35	ATICLLMQI	0.04%	98.73%	9
36	ATMCFLMQI	0.04%	98.77%	8
37	ATICFLIQI	0.04%	98.81%	8
38	ETVCFLMQI	0.03%	98.85%	7
39	GMANLVLQI	0.03%	98.88%	7
40	STTCFFMQI	0.03%	98.91%	7
41	GVISLMLQI	0.03%	98.95%	7
42	ATICFFMQI	0.03%	98.98%	6
43	GIASLMLQI	0.03%	99.01%	6

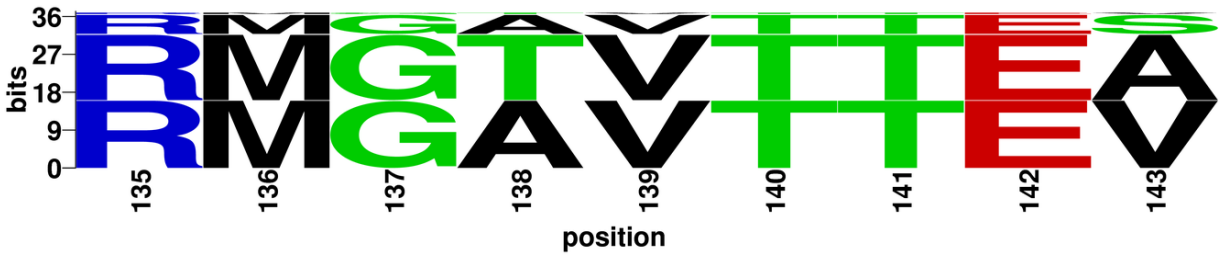

Peptide	HLA binding prediction							
	A*0101	**A*0201**	**A*0301**	**A*1101**	**A*2402**	**B*0702**	**B*0801**	**B*1501**
RMGAVTTEV	25911.28	28.24	8561.12	17804.25	8748.96	7567.75	11837.63	1814.06
RMGTVTTEA	29759.87	483.19	11819.71	18558.56	30110.63	15118.98	14058.85	3851.95
RMGAVTTES	36229.94	6509.78	11396.98	18507.23	30914.82	23274.96	26748.77	7346.77
RMGTVTTEV	26037.18	40.64	10979.87	19384.22	11265.07	9070.72	11882.79	2740.87

#	Peptide	Frequency	Accumulated frequency	Number of sequences
1	RMGAVTTEV	43.22%	43.22%	6501
2	RMGTVTTEA	42.03%	85.25%	6321
3	RMGAVTTES	12.74%	97.99%	1916
4	RMGTVTTEV	1.38%	99.38%	208

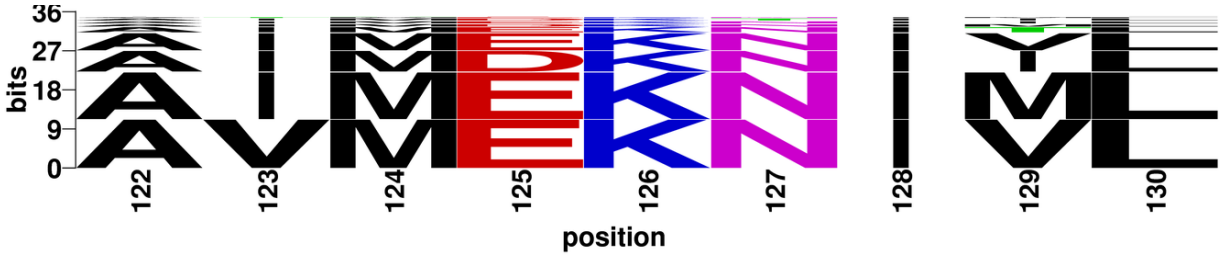

Peptide	HLA binding prediction							
	A*0101	**A*0201**	**A*0301**	**A*1101**	**A*2402**	**B*0702**	**B*0801**	**B*1501**
AVMEKNIVL	24979.71	269.9	16465.63	10402.78	21203.95	761.02	525.96	2102.57
AIMEKNIML	20535.84	55.15	14841.98	11096.19	20776.54	5052.68	792.18	5231.13
AIMDKNIIL	21552.3	167.31	16964.21	12334.61	26447.18	4809.75	1389.08	5021.5
AIMEKNIVL	23701.65	101.69	15605.61	12934.2	23016.52	2215.34	381.34	1609.79
AIMEKNITL	21926.75	40.1	14573.05	11838.77	16368.12	2526.58	309.84	2650.44
AIMDKNIML	20088.8	76.37	14749.2	9713.73	24521.2	4750.17	2101.98	5855.75

	5		9		6			
AIMEKNIIL	22241.2	141.36	16930.83	13770.26	23106.35	5176.07	539.05	4737.29
AIMDKTIIL	19337.3	75.41	10998.18	8012.85	21547.63	2744.58	769.57	2835.25
ATMEKNIML	7291.49	283.96	16026.91	5543.24	15537.22	5976.47	1884.6	7764.49
AITDKNIIL	25494.13	2971.47	27167.31	23022.5	36099.23	16485.42	12209.53	17499.06
AVMEKNIIL	23507.04	369.84	17686.37	11313.8	21768.61	2183.81	710.9	5652.25
AIMDKDIIL	23947.05	305.45	22101.1	17627.72	29394.08	8470.45	3204.68	5591.97
AAMEKNIVL	26609.62	3143.04	26571.95	20509.86	26761.79	945.8	379.2	4022.54
AVMEKNIML	21591.04	147.59	15503.3	8705.15	19417.8	2020.01	1062.16	6414.42
AIMEKSIML	21582.4	34.57	11216.66	9762.52	19171.06	4433.42	569.23	2730.63
VVMEKNIVL	23314.04	346.67	18904.92	16322.31	18847.53	1665.6	498.05	3123.17
AIMDKSIIL	23035.46	111.12	13232.17	11070.3	24717.05	4076.38	1006.16	2564.17
AIMGKNIML	24982.42	222.62	13485.83	11456.33	21694.78	4211.1	1612.86	6137.22
AIMDKVIIL	24161.51	51.45	12880.15	9813.46	23154.4	6035.08	964.59	2847.52
AIMDKAIIL	22625.17	204.52	14230.88	11145.05	26207.61	6113.29	1858.96	4141.83
AVMEKDIVL	27864.54	575.81	21965.93	15783.23	24744.61	1775.72	1347.95	2417.37
AIMGKNIIL	26202.51	405.37	15117.17	13980.59	23381.73	4262.21	1039.27	5262.24
AIMDKNITL	20909.6	46.19	14474.84	10546.6	19970.29	2272.12	794.02	2875.07
AVMGKNIVL	28551.51	662.55	15057.75	10073.81	21534.58	519.74	985.2	2290.51
AIMEKKIML	28595.11	322.72	16788.36	13979.07	25956.73	5870.34	447.12	9353.57
AVMDKNIIL	22793.74	433.01	17661.13	9763.05	24756.12	2068.18	1711.96	5942.17
AIMDKNVML	24822.37	112.42	18267.7	15145.17	22420.71	4755.72	1665.6	5215.31
AIMEKDIML	23093.61	105.46	20354.9	16839.66	23336.75	8464.41	1970.43	5611.43

#	Peptide	Frequency	Accumulated frequency	Number of sequences
1	AVMEKNIVL	31.23%	31.23%	3503
2	AIMEKNIML	30.22%	61.45%	3389
3	AIMDKNIIL	13.56%	75.01%	1521

4	AIMEKNIVL	11.31%	86.32%	1269
5	AIMEKNITL	3.80%	90.12%	426
6	AIMDKNIML	2.02%	92.15%	227
7	AIMEKNIIL	1.72%	93.87%	193
8	AIMDKTIIL	1.70%	95.57%	191
9	ATMEKNIML	0.93%	96.50%	104
10	AITDKNIIL	0.58%	97.08%	65
11	AVMEKNIIL	0.31%	97.39%	35
12	AIMDKDIIL	0.25%	97.64%	28
13	AAMEKNIVL	0.22%	97.86%	25
14	AVMEKNIML	0.17%	98.03%	19
15	AIMEKSIML	0.13%	98.16%	15
16	VVMEKNIVL	0.12%	98.28%	13
17	AIMDKSIIL	0.11%	98.39%	12
18	AIMGKNIML	0.07%	98.46%	8
19	AIMDKVIIL	0.07%	98.53%	8
20	AIMDKAIIL	0.06%	98.59%	7
21	AVMEKDIVL	0.06%	98.65%	7
22	AIMGKNIIL	0.06%	98.72%	7
23	AIMDKNITL	0.05%	98.77%	6
24	AVMGKNIVL	0.05%	98.82%	6
25	AIMEKKIML	0.05%	98.88%	6
26	AVMDKNIIL	0.04%	98.92%	5
27	AIMDKNVML	0.04%	98.97%	5
28	AIMEKDIML	0.04%	99.01%	5

References

1. Nielsen M*, et al.* (2007) NetMHCpan, a method for quantitative predictions of peptide binding to any HLA-A and -B locus protein of known sequence. *PloS one* 2(8):e796.
2. Ke Y*, et al.* (1988) Human bronchial epithelial cells with integrated SV40 virus T antigen genes retain the ability to undergo squamous differentiation. *Differentiation* 38(1):60-66.
3. Sykulev Y, Joo M, Vturina I, Tsomides TJ, & Eisen HN (1996) Evidence that a single peptide-MHC complex on a target cell can elicit a cytolytic T cell response. *Immunity* 4(6):565-571.
4. Ivanov AR, Zang L, & Karger BL (2003) Low-attomole electrospray ionization MS and MS/MS analysis of protein tryptic digests using 20-microm-i.d. polystyrene-divinylbenzene monolithic capillary columns. *Anal Chem* 75(20):5306-5316.
5. Reinhold B, Keskin DB, & Reinherz EL (2010) Molecular Detection of Targeted Major Histocompatibility Complex I-Bound Peptides Using a Probabilistic Measure and Nanospray MS3 on a Hybrid Quadrupole-Linear Ion Trap. *Analytical chemistry* 82(21):9090.
6. Kauppinen JK, Moffatt DJ, Mantsch HH, & Cameron DG (1981) Fourier Self-Deconvolution: A Method for Resolving Intrinsically Overlapped Bands. *Applied Spectroscopy* 35(3):271-276.